ขั้วไฟฟ้าดัดแปรด้วยแกรฟีนนาโนคอมพอสิตสำหรับการตรวจวัดทางเคมีไฟฟ้า

นางสาวชญาดา แสงสุกวาว

วิทยานิพนธ์นี้เป็นส่วนหนึ่งของการศึกษาตามหลักสูตรปริญญาวิทยาศาสตรมหาบัณฑิต
สาขาวิชาปิโตรเคมีและวิทยาศาสตร์พอลิเมอร์
คณะวิทยาศาสตร์ จุฬาลงกรณ์มหาวิทยาลัย
ปีการศึกษา 2557

GRAPHENE NANOCOMPOSITE MODIFIED ELECTRODE FOR ELECTROCHEMICAL DETECTION

Miss Chayada Saengsookwaow

A Thesis Submitted in Partial Fulfillment of the Requirements
for the Degree of Master of Science Program in Petrochemistry and Polymer Science
Faculty of Science
Chulalongkorn University
Academic Year 2014

Thesis Title	GRAPHENE NANOCOMPOSITE MODIFIED ELECTRODE FOR ELECTROCHEMICAL DETECTION
By	Miss Chayada Saengsookwaow
Field of Study	Petrochemistry and Polymer Science
Thesis Advisor	Professor Orawon Chailapakul, Ph.D.
Thesis Co-Advisor	Nadnudda Rodthongkum, Ph.D.
	Ratthapol Rangkupan, Ph.D.

Accepted by the Faculty of Science, Chulalongkorn University in Partial Fulfillment of the Requirements for the Master's Degree

.....Dean of the Faculty of Science
(Professor Supot Hannongbua, Dr.rear.nat)

THESIS COMMITTEE

.....Chairman
(Assistant Professor Warinthorn Chavasiri, Ph.D.)

.....Thesis Advisor
(Professor Orawon Chailapakul, Ph.D.)

.....Thesis Co-Advisor
(Nadnudda Rodthongkum, Ph.D.)

.....Thesis Co-Advisor
(Ratthapol Rangkupan, Ph.D.)

.....Examiner
(Associate Professor Voravee Hoven, Ph.D.)

.....External Examiner
(Associate Professor Weena Siangproh, Ph.D.)

ชญาดา แสงสุกวาว : ขั้วไฟฟ้าดัดแปรด้วยแกรฟีนนาโนคอมพอสิตสำหรับการตรวจวัดทางเคมีไฟฟ้า (GRAPHENE NANOCOMPOSITE MODIFIED ELECTRODE FOR ELECTROCHEMICAL DETECTION) อ.ที่ปรึกษาวิทยานิพนธ์หลัก: ศ. ดร.อรวรรณ ชัยลภากุล, อ.ที่ปรึกษาวิทยานิพนธ์ร่วม: ดร.นาฏนัดดา รอดทองคำ, ดร.รัฐพล รังกุพันธุ์, 71 หน้า.

งานวิจัยนี้ได้พัฒนาตัวรับรู้ทางเคมีไฟฟ้าโดยดัดแปรขั้วไฟฟ้าพิมพ์สกรีนคาร์บอนด้วยวัสดุนาโนคอมพอสิตของแกรฟีนสำหรับการตรวจวัดสารที่สนใจ (คอเลสเตอรอลและไฮดราซีน) โดยงานวิจัยแบ่งออกเป็น 2 ส่วน ส่วนแรกเป็นการดัดแปรขั้วไฟฟ้าพิมพ์สกรีนคาร์บอนด้วยวัสดุนาโนคอมพอสิตของแกรฟีน-พอลิไวนิลไพโรลิโดน/พอลิแอนิลีนสำหรับการตรวจวัดคอเลสเตอรอล ส่วนที่สองเป็นการพัฒนาขั้วไฟฟ้าพิมพ์สกรีนคาร์บอนที่ดัดแปรด้วยวัสดุนาโนคอมพอสิตของแกรฟีน-พอลิไวนิลไพโรลิโดน/อนุภาคนาโนของทองเพื่อเป็นตัวรับรู้ทางเคมีไฟฟ้าของไฮดราซีน ในงานวิจัยได้ศึกษาปัจจัยต่างๆ ที่มีผลต่อความไวในการตรวจวัดทางเคมีไฟฟ้าเช่น ส่วนประกอบของขั้วไฟฟ้าและตัวแปรทางเคมีไฟฟ้า โดยลักษณะทางกายภาพของขั้วไฟฟ้าดัดแปรสามารถศึกษาด้วยกล้องจุลทรรศน์แบบส่องกราดและกล้องจุลทรรศน์แบบส่องผ่าน ส่วนคุณสมบัติทางเคมีไฟฟ้าของขั้วไฟฟ้าดัดแปรสามารถศึกษาด้วยเทคนิคไซคลิกโวลแทมเมตรีและเทคนิคอิเล็กโตรเคมิคอล อิมพิแดนซ์ สเปกโทรสโกปี จากผลการวิจัยพบว่าขั้วไฟฟ้าดัดแปรมีความไวในการตรวจวัดสูงขึ้นเมื่อเทียบกับขั้วไฟฟ้าที่ไม่ได้ดัดแปร ภายใต้สภาวะที่เหมาะสมพบว่า ขั้วไฟฟ้าดัดแปรแสดงขีดจำกัดในการตรวจวัดที่ต่ำ มีความไวในการตรวจวัดสูงและมีช่วงความเข้มข้นในการตรวจวัดกว้าง นอกจากนี้ยังมีการศึกษาความจำเพาะในการตรวจวัดสารเมื่อมีตัวรบกวนและระบบขั้วไฟฟ้าดัดแปรได้ถูกนำไปประยุกต์ใช้ในการตรวจวัดสารในตัวอย่างจริงได้

สาขาวิชา ปิโตรเคมีและวิทยาศาสตร์พอลิเมอร์ ลายมือชื่อนิสิต .....

ปีการศึกษา 2557 ลายมือชื่อ อ.ที่ปรึกษาหลัก .....

ลายมือชื่อ อ.ที่ปรึกษาร่วม .....

ลายมือชื่อ อ.ที่ปรึกษาร่วม .....

5472231223 : MAJOR PETROCHEMISTRY AND POLYMER SCIENCE
KEYWORDS: GRAPHENE / POLYVINYLPYRROLIDONE / GOLD NANOPARTICLE / ELECTROSPRAYING / CHOLESTEROL / HYDRAZINE

CHAYADA SAENGSOOKWAOW: GRAPHENE NANOCOMPOSITE MODIFIED ELECTRODE FOR ELECTROCHEMICAL DETECTION. ADVISOR: PROF. ORAWON CHAILAPAKUL, Ph.D., CO-ADVISOR: NADNUDDA RODTHONGKUM, Ph.D., RATTHAPOL RANGKUPAN, Ph.D., 71 pp.

The electrochemical sensors based on graphene nanocomposite modified screen-printed carbon electrode (SPCE) were prepared for the determination of target analytes (*e.g.* cholesterol, hydrazine). This study is separated into two main parts. The first one is using graphene-polyvinylpyrrolidone/polyaniline nanocomposite (G-PVP/PANI) modified SPCE for the determination of cholesterol. The second one is development of nitrogen-doped graphene-polyvinylpyrrolidone/gold nanoparticles (NG-PVP/AuNPs) modified SPCE as a novel electrochemical sensor for hydrazine. The factors affecting the electrochemical sensitivity of the systems, such as electrode composition and electrochemical parameters were evaluated. Scanning electron microscopy and transmission electron microscopy were used for physical characterization of modified SPCE. The electrochemical behaviors of the modified SPCE were examined by cyclic voltammetry and electrochemical impedance spectroscopy. The modified SPCEs showed the improved electrochemical sensitivities compared to unmodified SPCE. Under optimum conditions, the modified SPCEs exhibited a low detection limit, a high sensitivity and a wide linearity. Moreover, the selectivity of modified SPCEs in the presence of common interferences was investigated. Ultimately, the modified SPCEs were successfully applied for the sensitive determination of target analytes in real samples.

Field of Study:	Petrochemistry and Polymer Science	Student's Signature .....
		Advisor's Signature .....
Academic Year:	2014	Co-Advisor's Signature .....
		Co-Advisor's Signature .....

ACKNOWLEDGEMENTS

I would like to thank all my thesis advisor and co-advisors including Professor Dr. Orawon Chailapakul, Dr. Nadnudda Rodthongkum and Dr. Ratthapol Rangkupan for their useful advices and encouragement throughout the thesis.

I am grateful to all the thesis committee members including Assistant Professor Dr. Warinthorn Chavasiri, Associate Professor Dr. Voravee Hoven and Associate Professor Dr. Weena Siangproh for their comments and interested advices.

I would like to appreciate the financial supports from the Ratchadaphiseksomphot Endowment Fund and the National Nanotechnology Center (NANOTEC), NSTDA, Ministry of Science and Technology, Thailand.

I am also thankful for the warm friendship and great motivation from all my group members.

Finally, I would like to thank my family for their love and encouragement throughout my entire life.

CONTENTS

Page

Page

Page

Page

Page

Page

LIST OF TALBLES

Page

LIST OF FIGURES

Page

CHAPTER I
INTRODUCTION

1.1 Introduction

Electrochemical sensor has been widely used in various fields of applications owing to its simplicity, rapid response, high sensitivity and portability. To prepare the electrochemical sensor, screen printing technique has been used to fabricate small electrode instead of using large-scale conventional electrode, such as gold electrode, graphite pencil electrode and glassy carbon electrode. Screen-printed carbon electrode (SPCE) is uniquely qualified for meeting the ease of use, small size and low cost, so it has been emerged as an effective tool for electrochemical sensor application [1, 2]. Compared with large-scale conventional electrode, small size of SPCE is more compatible with limited amount of sample and it also reduces the amount of waste. Nevertheless, due to the small size of electrode, the surface area of working electrode exposed to the sample is limited leading to the decreased electrochemical sensitivity of the system. To overcome this problem, modification of working electrode surface is highly required to increase the surface area in the development of sensitive electrochemical sensor.

Nanostructured materials (*e.g.* carbon based nanomaterials and metallic nanoparticles) have been used for electrode surface modification to improve the electrochemical sensitivity. Graphene (G) is a flat monolayer of sp^2 hybridization carbon atom arranged in two-dimensional honeycomb crystalline lattice [3, 4]. G-based nanomaterials become a promising material for electrode surface modification due to its high surface area, excellent electrical conductivity, high mechanical strength and good biocompatibility. G-based electrodes offer the high sensitivity in the detection of various chemicals [5, 6] and biomolecules [7-9]. With the chemical doping strategy, insertion of foreign atoms into the carbon structures is an effective method for adjusting the electrochemical and surface properties of G [10]. Recently, it was reported that chemical doping of G with heteroatom (*i.e.* nitrogen) can promote the catalytic activity in electrochemical reduction of hydrogen peroxide and

accelerate the electron transfer for glucose oxidase in electrochemical sensor application [11]. However, owing to their flat sp^2-carbon structure, G-based nanomaterials have high tendency to agglomerate or restack together to form graphite through the Van der Waals interaction leading to the deficiency of their unique properties [12]. To obtain the pure form of G, polyvinylpyrrolidone (PVP) has been used as a stabilizer to prevent the agglomeration of G in organic solvents [13]. Along with PVP, G showed the good electrocatalytic activity toward the reduction of O_2 and H_2O_2 in biosensor application [14].

Moreover, the nanocomposite of G and conducting polymer is more suitable than the pure form of G for electrode surface modification and further functionalization with biomolecules. Among conducting polymers, polyaniline (PANI) has become a promising material, owing to its high electrical conductivity, simply synthesis, and biocompatibility [15]. Moreover, PANI possesses a large number of amino groups which can be used for functionalization with biomolecules in biosensor applications.

Also, metallic nanoparticles have received much attentions in the electrochemical applications because of their superior properties (*e.g.* large effective surface area, extraordinarily catalytic activity and high conductivity) than bulk metals [16]. Particularly, gold nanoparticles (AuNPs), which have high conductivity, electrocatalytic activity and good biocompatibility, have been used in the electrode surface modification for electrochemical detection of various analytes [17-19].

For electrode surface modification using nanostructure materials, several modification methods have been employed, such as drop casting [14, 20], ink-jet printing [21], electrodeposition [16, 22] and electrospinning [23-25] and electrospraying [26, 27]. In this study, electrospraying was selected because it can create 3D droplet-like nanostructures of the nanocomposites on the electrode surface by applying high voltage of electric field. The large surface area of nanodroplet modified electrode leads to enhanced electrochemical sensitivity of the electrode in electrochemical sensors [26]. Moreover, metal electrodeposition was applied for the electrode surface modification. Electrochemical deposition of metal

can provide a thin and tightly adhesive of desired metal on a substrate surface by using electrolysis of metal solution. In an appropriate condition, the nanoparticles of desired metal can be generated on the electrode surface with high surface area resulting in the improved electrochemical sensitivity.

Development of novel sensors, which provide rapid, sensitive, inexpensive and convenient determination of biomolecules and chemicals, is crucial for various fields of applications including biomedical analysis, food quality control, forensic science, as well as environmental monitoring. Recently, the target of analytes (*e.g.* clinical biomarker and food contaminant) have received more interest in the development of novel electrochemical sensor and biosensor because the abnormal level of these compounds can cause the serious effect on human health. Therefore, the development of effective method for sensitive detection of desired biomarkers and food contaminants is still greatly required.

In this work, the novel electrochemical sensor based on graphene nanocomposite modified SPCE were developed for the sensitive determination of biomolecule and chemical. The factors affecting analytical performances of electrochemical sensor were optimized and then applied for the electrochemical determination of target biomolecule or chemical in real samples. The presentation of development of electrochemical sensor in this thesis consists of 2 main parts as followings:

1. Graphene-Polyvinylpyrrolidone/Polyaniline Nanocomposite Modified Electrode for the Determination of Cholesterol
2. Nitrogen-Doped Graphene-Polyvinylpyrrolidone/Gold Nanoparticles Modified Electrode as a Novel Hydrazine Sensor

1.2 Objectives

- To prepare graphene nanocomposite modified screen-printed carbon electrode (SPCE)
- To use fabricated sensor for the electrochemical detection of target analytes in real samples.

1.3 Scope of the research

In this study, the electrochemical sensor based on graphene nanocomposite modified screen-printed carbon electrode (SPCE) was prepared for the determination of target analytes. The factors exhibiting a profound influence on the electrochemical responses of target analytes were investigated and optimized. Moreover, the analytical performances of modified SPCE for electrochemical detection including a linear range, a detection limit, selectivity and stability were evaluated. Finally, the optimum conditions were applied for the determination of target analytes in real samples.

CHAPTER II

THEORY AND LITERATURE SURVEY

In this chapter, the basic principles of electrochemical detection are described. In the second part of this chapter, techniques used for electrode fabrication and the materials employed for electrode surface modification in this study are introduced. The third part focuses on the electrode modification processes (*i.e.* electrospraying and electrodeposition). Eventually, the importance of the target of analytes (*e.g*. cholesterol and hydrazine) is discussed.

2.1. Electrochemical methods

Electrochemical methods have been extensively used in the development of sensors as the detection and characterization protocols. These methods are involved with the measurement of electrical quantities (*e.g*. current, potential or charge) related to the chemical parameters taking place at the electrode-solution interface. In an electrochemical cell, at least 2 electrodes and electrolyte solution are required. For electrochemical measurement, a working electrode (WE) is applied for the detection of electroactive species and a reference electrode (RE) with a constant potential is independent from the properties of measured solution. In some electrochemical techniques, a counter electrode is also used to balance the current observed at a working electrode [28].

In general, the electrochemical measurements are classified into two types (*e.g.* potentiometric and potentiostatic). Potentiometry is a static (zero current) technique that is based on the measurement of the potential between working electrode and reference electrode. Potentiostatic (controlled-potential) technique is based on a dynamic technique (no zero current) that measure the current response obtained from electron transfer process while the working electrode is applied with controlled potential. The applied potential can cause an oxidation and reduction (redox reaction) in which the electroactive species receive and lose an electron across the electrode-solution interface. The current response obtained from

potentiostatic technique is directly related to the concentration of electroactive species (target analytes) in measured solution. The redox reaction of target analyte at electrode-electrolyte interface is described below (equation 2.1):

$$O + ne^- \longleftrightarrow R \qquad (2.1)$$

Where O and R are the oxidized and reduced forms of electroactive species, respectively. This redox reaction can be achieved when the system is applied with the potential making electron transfer thermodynamically or kinetically favorable. For thermodynamic electron transfer process, the relationship between the applied potential and the concentration of electroactive species can be expressed as a Nernst equation shown below (equation 2.2) [28]:

$$E = E^o + \frac{2.3\ RT}{nF} log \frac{C_o(0,t)}{C_R\ (0,t)} \qquad (2.2)$$

Where E^o = standard potential of redox process

R = molar gas constant (8.314 K/mol)

T = Kelvin temperature

n = number of transferred electrons

F = Faraday constant (96,487 coulombs)

C_o, C_R = concentration of oxidized species and reduced species, respectively

For the development of electrochemical sensor, the potentiostatic techniques including cyclic voltammetry (CV), square wave voltammetry (SWV) and amperometry were employed for the determination of target analytes in this work. To characterize the interfacial properties of fabricated sensor, the developed sensor was characterized by the electrochemical impedance spectroscopy (EIS). The basic principle of these techniques will be discussed in the next part.

2.1.1 Cyclic voltammetry (CV)

Cyclic voltammetry (CV) is the most extensively used techniques for electrochemical characterization of electrochemical process providing the information about thermodynamics, kinetics and coupled chemical reaction or adsorption processes. Especially, it can provide a potential for redox process of electroactive species and evaluation of media effect on redox reaction.

For CV measurement, the linear sweeping of potential with triangular waveform (Figure 2.1A) is applied to working electrode, while the resulting current is measured to provide the plot in term of "cyclic voltammogram" as an output (Figure 2.1B). The potential is scanned in forward and backward direction with the same scan rate. When the potential is swept forward to negative-side potential and reached at the standard potential of redox process (E^0), the reduction process is occurred to obtain the R form of electroactive species and a cathodic peak. On the other hand, in the backward scan, the R form is oxidized (oxidation process) to generate O form and anodic peak [28].

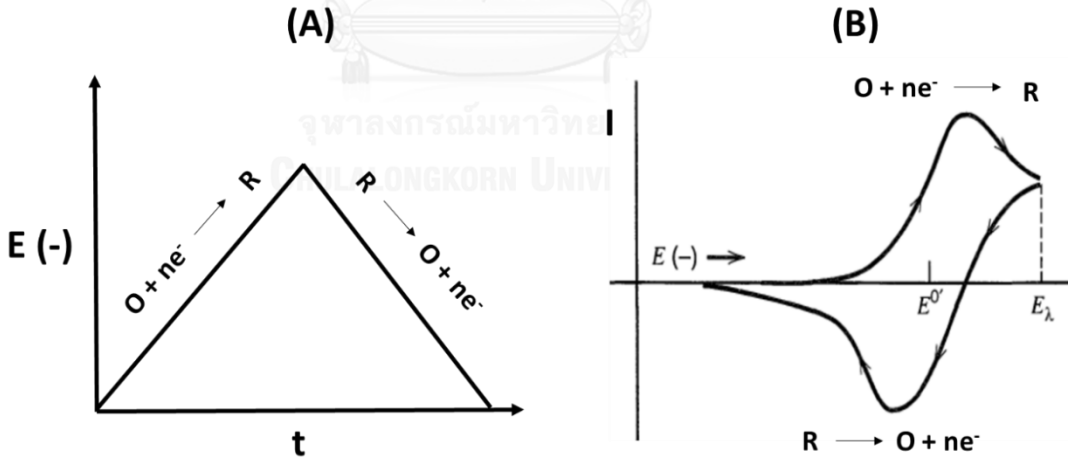

Figure 2.1 (A) Applied potential-time profiles in cyclic voltammetric measurement and (B) cyclic voltammogram of a reversible redox process [29].

2.1.1.1 Reversible system

For reversible system, the relationship between anodic peak current ($I_{p,a}$) or cathodic peak current ($I_{p,c}$) versus the scan rate is given by Randle-Sevcik equation as shown in equation 2.3 [28]:

$$I_p = (2.69 \times 10^5)\, n^{3/2} ACD^{1/2} \nu^{1/2} \quad (2.3)$$

Where n = number of transferred electrons

A = electrode surface area (cm^2)

C = concentration of electroactive species

D = diffusion coefficient ($cm\ s^{-1}$)

ν = scan rate ($V\ s^{-1}$)

In general, the peak current is measured by subtracting with baseline current. For a simple reversible couple, the ratio of cathodic-to-anodic peak current ($I_{p,c}/ I_{p,a}$) is unity. The formal potential (E^0) is located at the halfway between the anodic peak potential ($E_{p,a}$) and cathodic peak potential ($E_{p,c}$) with the relationship of equation 2.4. The peak potential difference (ΔE_p) can be used for the determination of electron number using the equation 2.5

$$E^0 = (E_{p,a} + E_{p,c})/2 \quad (2.4)$$

$$\Delta E_p = E_{p,a} - E_{p,c} = (0.059/n)V. \quad (2.5)$$

2.1.1.2 Irreversible and quasi-reversible systems

For totally irreversible system, the widely separated peaks can be observed. The relationship of peak potential and scan rate is expressed by equation 2.6 [29]:

$$I_p = (2.99 \times 10^5)^{1/2}) \alpha^{\alpha^{1/2}} ACD^{1/2} \nu^{1/2} \quad (2.6)$$

Where the α is related to the equation 2.7:

$$| E_p - E_{p/2} | = 47.7/^{\alpha}\alpha \text{ at } 25\ ^{\circ}C \quad (2.7)$$

Where $E_{p/2}$ is the potential at half peak current

For quasi-reversible system, the peak current is depended on both charge transfer and mass transfer process. The anodic and cathodic peak potential of this system are larger separated than that of reversible system.

2.1.2 Square wave voltammetry (SWV)

Square wave voltammetry (SWV), is one of a pulse techniques, has been received much attention as a high performance technique providing quantitative information of target analyte. SWV technique is based on applying potential with staircase waveform where the forward pulse is coincident with the staircase step and reverse pulse is occurred in half way potential of the staircase step as shown in Figure 2.2A. The current of this method is sampled twice (at the end of forward and reverse pulse) obtaining the output called "square wave voltammogram" as seen in Figure 2.2B. The shape of resulting current is symmetrical and current response is proportional to the concentration of target analytes. The speed of the SWV measurement can be easily controlled by the effective scan rate. Moreover, The SWV measurement shows the faster response and higher sensitivity than normal pulse and differential pulse techniques [28].

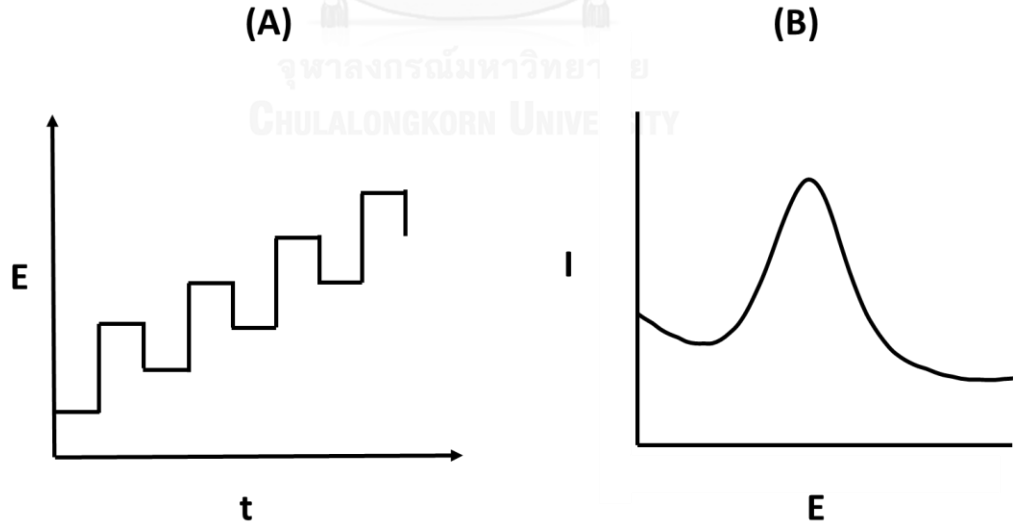

Figure 2.2 (A) Applied potential-time profiles in square wave voltammetric measurement and (B) square wave voltammogram of electroactive species.

2.1.3 Chronoamperometry

Chronoamperometry is a one of the potentiostatic techniques which the fixed-value potential is applied to the working electrode (Figure 2.3A) at a value where the electroactive species undergo either oxidation or reduction. Consequently, the current response is measured as a function of time (Figure 2.3B). This technique is performed in stationary working electrode and unstirred solution system. Generally, the current response of this method is proportional to the concentration of analyte. This technique is usually applied for investigating an electrode surface area and diffusion coefficient of target analyte [28, 29].

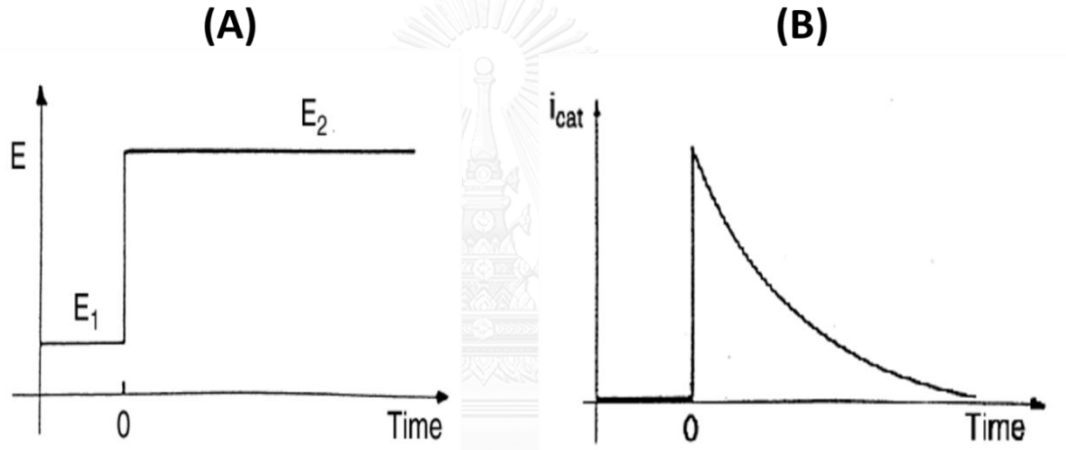

Figure 2.3 (A) Applied potential-time profiles in amperometric measurement and (B) chronoamperogram of electroactive species [28].

2.1.4 Electrochemical impedance spectroscopy (EIS)

Electrochemical impedance spectroscopy (EIS) is an effective technique for investigation of electrochemical reaction mechanism, and dielectric and insulating feature of materials. The concept of EIS method is based on the electrical perturbation of physic-electrochemical system by applying an alternating current (ac) to the electrical circuit. The electrochemical impedance is measured as a function of frequency. The plot of impedance versus frequency is called “Nyquist plot” as shown in Figure 2.4. For EIS interpretation, the semicircle diameter is represented to the electron transfer resistance (R_{ct}) of the measured electrochemical cell [29, 30].

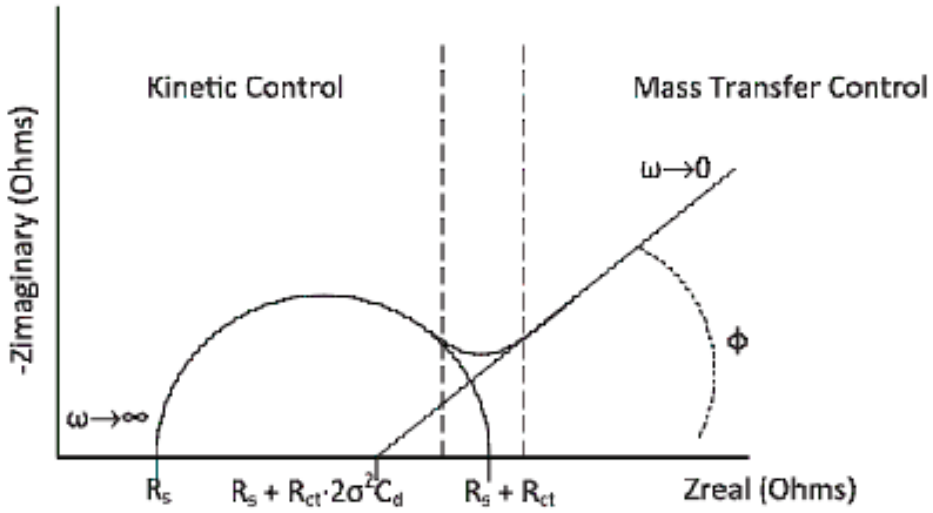

Figure 2.4 Typical electrochemical impedance spectrum in term of Nyquist plot [31].

2.2 Screen-printing technique

With the advent of screen-printing technology, the practical application of electrochemical techniques for the medical diagnosis at point-of-care and environmental analysis outside a laboratory have been achieved. The screen-printing technique can be used for fabrication of the screen-printed electrodes (SPEs) in mass production.

For the fabrication of SPEs, a woven mesh supported an ink-blocking stencil is used, then conductive ink is forced or pumped through the mesh and attached onto a desired substrate (Figure 2.5). The configuration of SPEs is flexible for compatibility with the specific analytes. Moreover, this technique is very convenient to use as an in-house method for SPE fabrication in small batch. Therefore, SPEs may be the most appropriate electrochemical sensors for in situ analysis because of their advantages including low power requirement, disposability, ease of surface modification, changeability of electrode configuration design and ability to operate at room temperature [32].

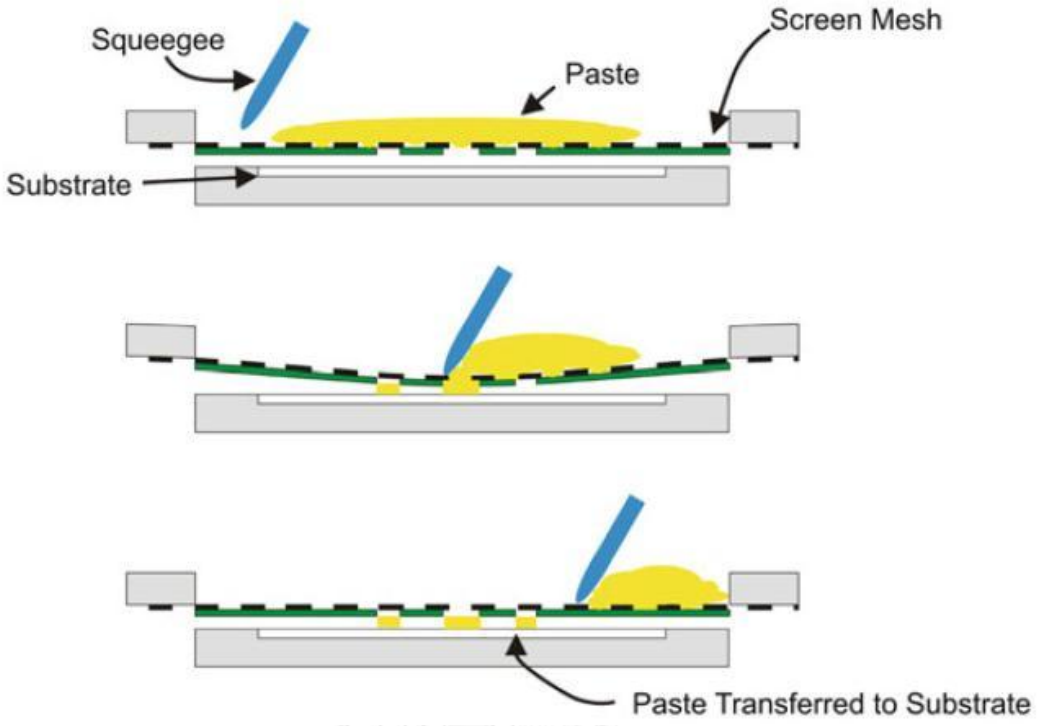

Figure 2.5 Schematic representation of the screen-printed manufacturing process (cross-sectional side view) outlining the basic processes involved for the production of electrochemical sensors [33].

However, the printing inks for the SPEs fabrication contain some mineral binders or insulating polymers for the adhesion onto the substrate. These insulating materials may shield the electrochemical activity of carbon particles in working electrode and cause the slow kinetics of electron transfer resulting in the decrease of electrochemical sensitivity of screen-printed carbon electrodes (SPCEs). Moreover, the limited surface area of SPCE, which is caused by the fact that the SPCEs is usually designed to be a small size for the compatibility with using outside the laboratory and with limited amount of sample This is one of the reasons that leads to decreased electrochemical sensitivity of the system. Thus, the electrode surface modification has been extensively required to improve the sensitivity of electrochemical sensors.

2.3 Electrode surface modification

The conventional electrochemical sensor consists of three electrodes including reference electrode (RE), counter electrode (CE) and working electrode (WE) which are immersed in an electrolyte solution containing target analyte. As mention in the last section, the WE, at which the electrochemical reaction of analyte is occurred, is the important part that directly indicates the sensitivity of electrochemical system.

In this section, various nanomaterials, such as carbon-based materials (*e.g.* carbon nanotube, graphene), metallic nanomaterial (*i.e.* gold nanoparticles), and conducting polymer (*i.e.* polyaniline) used for modification of WE surface will be described. Moreover, the surface modification techniques (*i.e.* electrospraying and electrodeposition) for improved electrochemical sensitivity will be explained.

2.3.1 Nanomaterials used for electrode surface modification

2.3.1.1 Carbon-based nanomaterials

Carbon-based materials are confined as an ideal electrode substrate because carbon electrode can offer low residue current, wide anodic potential range, fast response and ease of fabrication. Recently, with the advent of nanotechnology, carbon-based materials such as carbon nanotube (CNT) and graphene (G) have been extensively used for electrode surface modification due to their high electrochemical conductivity and large surface area leading to improved electrochemical sensitivity of modified electrode. However, the limitation of CNT is the contamination of residual metallic impurity during the synthetic process even after multiple purification steps. Using CNT-based electrode, the existence of the metallic impurity can cause the misinterpretation of electrochemical results and affect the reproducibility of the system [34]. To overcome this problem, graphene (G) was introduced as a promising material for electrode surface modification instead of CNT.

Graphene (G) is a flat monolayer of sp^2 hybridization carbon atom arranged in two-dimensional honeycomb crystalline lattice. G has superior properties compared with CNT in term of the low cost, high electrocatalytic activity, high electrical

conductivity and large surface area. Therefore, G becomes a material of interest in various applications. Moreover, the insertion of heteroatom (*i.e*. nitrogen) into the carbon structures is an effective method for adjusting the electrochemical and surface properties of G [10]. However, the use of G has a problem with the self-agglomeration of G via Van der Waals and **π-π** interactions resulting in the decrease of its electrochemical activity. Recently, polyvinylpyrrolidone (PVP) have been used as a stabilizing polymer to improve the dispersion of G in organic solvent [13, 14].

Shan, C *et al* [14] was developed the glucose biosensor based novel polyvinylpyrrolidone-protected graphene/polyethylenimine-functionalized ionic liquid modified electrode. This fabricated electrode showed an electrochemical reduction toward O_2 and H_2O_2, and exhibited a linear response for the glucose detection up to 14 mM.

2.3.1.2 Polyaniline (PANI)

Various conducting polymers, including polyaniline (PANI) [17, 23], polypyrrole (PPy) [35, 36] and poly(3,4-ethylenedioxythiophene) (PEDOT) [37, 38] have been applied in electrochemical sensors. Among conducting polymers, PANI has been gained much attention, owing to its high conductivity, simple synthetic procedures, high environmental stability and good biocompatibility [15]. Moreover, PANI possesses a large number of amino groups, which can be used for functionalization with biomolecules (*e.g.* enzyme, nucleic acids, antibodies, etc.) in biosensor applications. PANI has three basic forms including leucoemeraldine (LE), pernigraniline (PG) and emeraldine base (EB). The form of EB is considered as the most useful of form of PANI owing to its high stability and it can be doped with acid to form emeraldine salt (ES) possessing electrical conductivity through its **π-π** conjugated bond (Figure 2.6). However, LE and PG forms have poor conductivity even after doping with an acid [15].

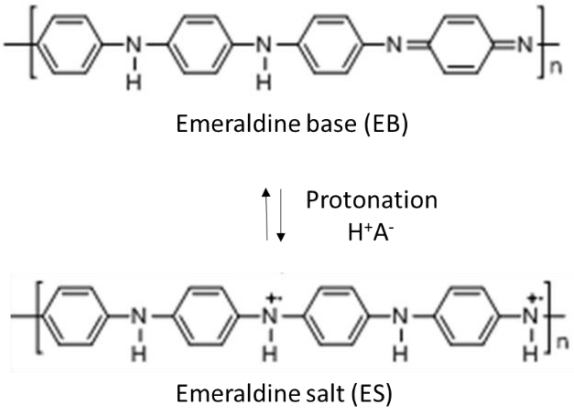

Figure 2.6 The form of polyaniline during the protonation of emeraldine base (insulator) and emeraldine salt (conductor).

Recently, it has been reported that the nanocomposites of G/PANI significantly enhance both electrochemical conductivity and electrocatalytic activity of modified electrodes [9, 20, 24, 39]

Fan, Y *et al.* [20] developed an electrochemical sensor based on graphene–polyaniline (G–PANI) nanocomposite modified glassy carbon electrode for the determination of 4-aminophenol (4-AP). The fabricated sensor exhibited a low detection limit of 6.5 $\times 10^{-8}$ M and a high sensitivity of 604.2 μA mM^{-1}. Moreover, it could be used for simultaneous detection of 4-AP and paracetamol without interference effect.

Lui, S *et al.* [9] developed graphene–polyaniline (G–PANI) nanocomposite film modified glassy carbon for dopamine (DA) detection. The dopamine aptamer was chemically immobilized onto G-PANI film to create a label-free electrochemical aptasensor. This developed aptasensor showed a low detection limit of 0.00198 nM and could be apply for DA determination in human serum.

2.3.1.3 Gold nanoparticles (AuNPs)

Metal nanoparticles have emerged as materials of interest due to their unique physical (*e.g.* physical, electronic magnetic and optical) and chemical (*i.e.* catalytic) properties. Their properties depend on their size, shape and stabilizing agent controlling by preparation method. Particularly, gold nanoparticles (AuNPs), which

have high electrical conductivity, excellent electrocatalytic activity and large surface area, have been applied for electrode surface modification for electrochemical sensor. Moreover, they have a good biocompatibility which can be immobilized with biomolecules without loss of bioactivity. [40, 41].

Bernalte, E. *et al.* [18] used commercial gold nanoparticles modified screen-printed carbon electrode (AuNPs-SPCEs) to develop a simple, fast and cheap method for the determination of Hg(II). This method could measure the concentration of Hg(II) in low level (ppm range) and could be applied for Hg(II) detection in real ambient water samples.

Furthermore, nanocomposite of graphene and gold has been used for electrode modification to improve the electrochemical sensitivity. Pruneanu, S., *et al.* [19] fabricated electrochemical sensor for the determination of carbamazepine (CBZ) using a novel graphene-gold nanoparticles (G-AuNPs) modified gold electrode. The results showed that this fabricated sensor exhibits 2-fold increase in peak current intensity and a strong electrocatalytic activity toward the carbamazepine oxidation.

2.3.2 Electrode modification techniques

2.3.2.1 Electrospraying technique

Electrospraying is an electrical-based technique that is used for the preparation of small particles in a scale of micro to nanometers. This technique is slightly modified from electrospinning technique, used for fabricating micro/nanofibers. For electrospraying technique, a high electric field is applied to needle tip of a syringe containing a polymer solution. Assuming a positive potential, positive charge in the polymer solution will accumulate at the surface and then the solution forms a cone-like shape called “Taylor cone”. When the applied potential is high enough, the cone will be drawn out through a “budding process” and then resulting in the positively charged droplets (Figure 2.7). The difference between electrospraying and electrospinning is the concentration of polymer that is used in the process. For the fabrication of fibers, high concentration of polymer is required in the electrospinning process. On the other hand, electrospraying is used a relatively

low concentration of polymer to form a small droplets. The factors that affect the diameter of sprayed droplets are included an applied potential, a flow rate of polymer solution, a concentration of polymer and solvent properties [42, 43].

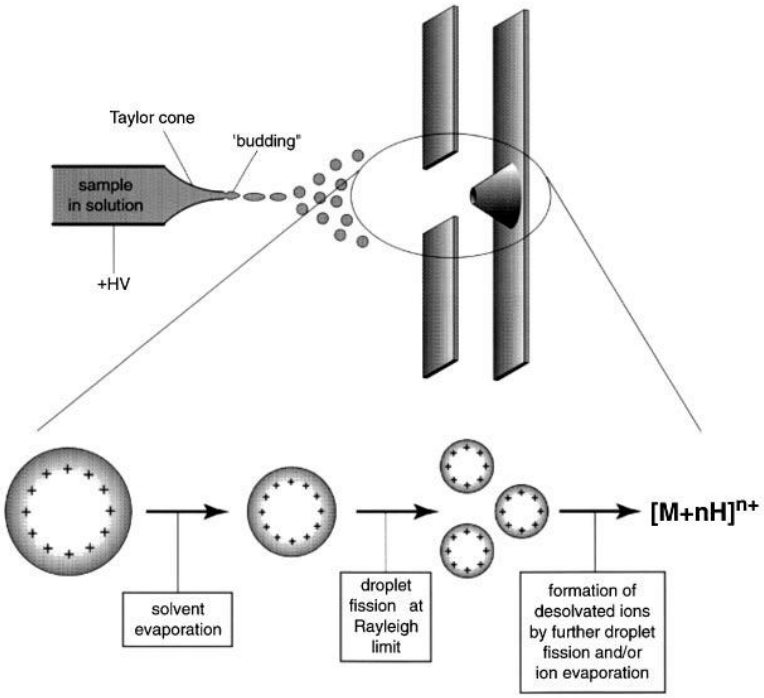

Figure 2.7 The formation of small droplets produced by electrospraying process [43].

For the application of electrospraying in electrochemical sensor, electrospraying process can provide nanodroplets of desired materials generated onto electrode surface. The large surface area of nanodroplets leads to the increase in electrode surface area and resulting in the improved electrochemical sensitivity of the modified electrode compared to thin film modified electrode. Moreover, the high surface area of the nanodroplets modified electrode provides more active surface in biosensor applications.

Reucha, N *et. al.* [39] used the electrospraying technique to fabricate the nanodroplets of graphene/polyvinylpyrrolidone/polyaniline (G/PVP/PANI) nanocomposite onto the paper-based electrode for the determination of cholesterol. The nanodroplets were uniformly generated on electrode surface with average size of 160 ± 1.02 nm as shown in Figure 2.8. Under optimum conditions, this

developed biosensor exhibited a low detection limit and wide linear range and could be successfully applied for the cholesterol detection in human serum.

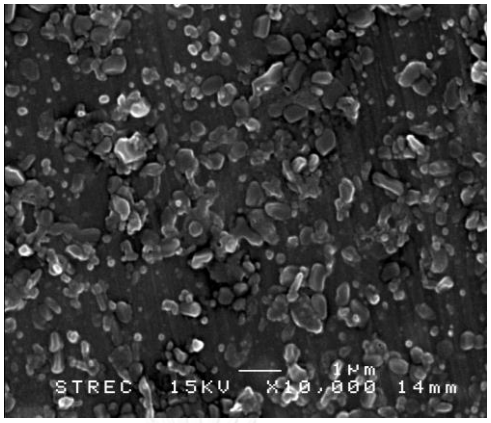

Figure 2.8 SEM image of G/PVP/PANI nanodroplet modified electrode [39].

2.3.2.2 Electrodeposition technique

Electrochemical deposition of metal can provide a thin and tightly adhesive of desired metal on a substrate surface by using electrolysis of metal solution. The deposited metals can be formed as nanocrystallines, nanowires, nanotubes, nanomultilayers, nanocomposites and nanoparticles (Figure 2.9). In this study, metal electrodeposition was applied for the electrode surface modification because the nanoparticles of desired metal can be generated on the electrode surface with high surface area resulting in the improved electrochemical sensitivity of the system.

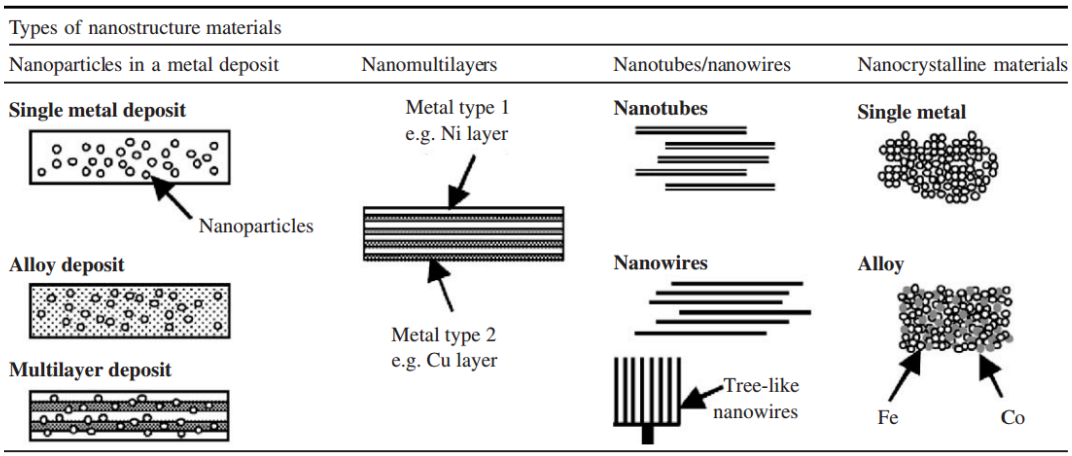

Figure 2.9 Various types of nanostructured materials which may be produced by electrodeposition technique [44].

2.4 Biosensors

Biosensors are electronic devices that provide quantifiable electrical signal using bio-receptors, based on affinity between complementary structures, such as enzymes, antibodies, nucleic acid, cells, receptor protein, etc., and electronic transducer coupled with amplifier (Figure 2.10). Recently, biosensor has attracted great interest because of its potential application in clinical diagnosis and bioprocess monitoring. In general, biosensor is composed of three main parts: **(1) a recognition part** in which the bio-receptors are immobilized on a solid surface for a target analyte recognition, **(2) a transducer or a detector element**, which convert the interaction between the target analyte and the bio-receptor into another signal that can be easily quantified, **(3) a signal processor or an associated electronic** that is primarily responsible for the display of the output signal in a user-friendly way. For the analysis of target analyte, the quantity of output signal is proportional to the concentration of the analyte providing both quantitative and qualitative information [15, 45].

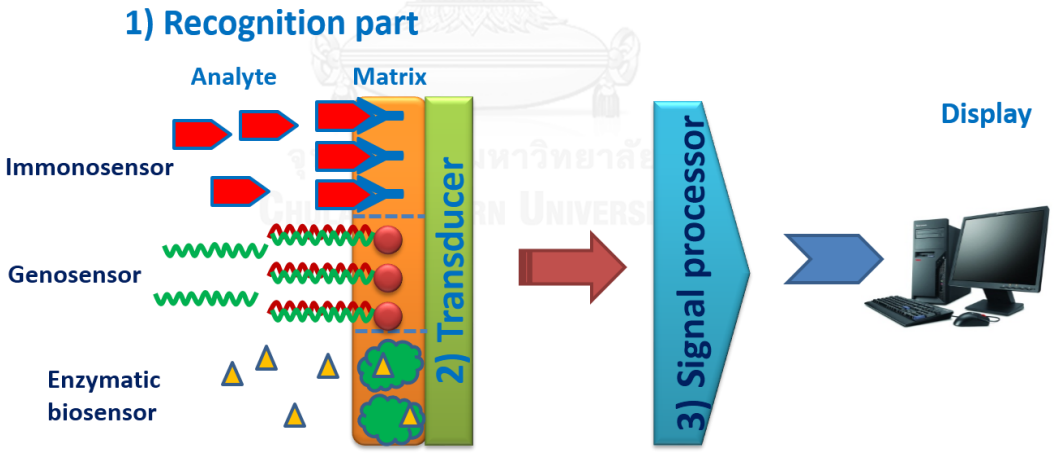

Figure 2.10 Schematic diagram of biosensor component [15]

Biosensors can be categorized into various types depending on transducer mechanism including resonant biosensors, optical-detection biosensors, thermal-detection biosensors, ion-sensitive FET biosensors and electrochemical biosensors [34, 46].

2.5 Target analytes

The clinical biomarkers and food contaminants that can cause the serious effects in the human health have been increasing interested. In this work, biomarker (*i.e.* cholesterol) and toxic food contaminant (*i.e.* hydrazine) are focused.

2.5.1 Cholesterol

Cholesterol and cholesterol ester are the main molecules found in cell membrane of both humans and animals, and act as the precursors of other biological reagents (*e.g.* steroid hormone and bile acid). It is made by the liver and also being in dietary intake of fats. [45, 47]. Its content in normal human blood plasma is about 130-260 mg dL^{-1}, one-third of which is sterol and two-third is esterified with fatty acid [35]. The abnormal cholesterol level in blood may cause lipid metabolism disorder. Many researches of medicine reported that a high total cholesterol level (the sum of free cholesterol and cholesterol esters) is involved in cerebral thrombosis, arteriosclerosis and coronary heart diseases. On the other hand, hyperthyroidism, malabsorption, anemia and wasting syndromes are found in the patients with the lack of cholesterol [48]. Thus, the determination of cholesterol level is very crucial in clinical diagnosis.

For electrochemical determination of cholesterol, the enzymatic bioassay is preferred to chemical reaction due to its high specificity and selectivity. The electrochemical biosensor for cholesterol detection is usually based on the monitoring of the consumption of oxygen or the production of hydrogen peroxide which are caused by enzymatic reaction as shown in Figure 2.11.

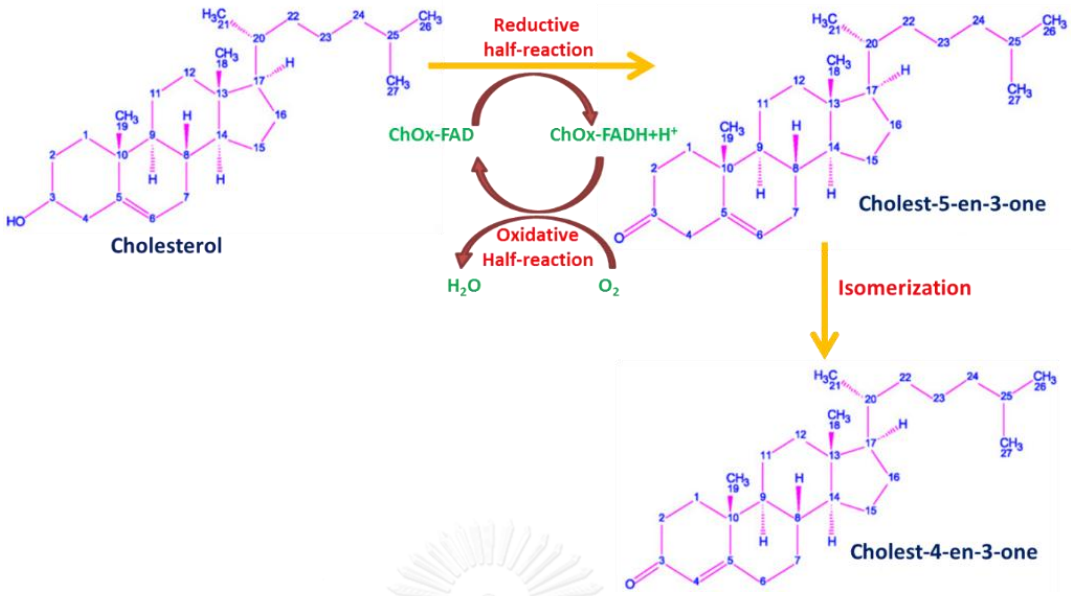

Figure 2.11 Pathway of reaction catalyzed by cholesterol oxidase enzyme [45].

Soylemez et al. [49] developed an amperometric cholesterol biosensor based on a novel matrix 2-(4-fluorophenyl)-4,7-di(thiophene-2-yl)-1*H*-benzo[d]imidasole (BIPF). Due to the strong **π–π** interaction of aromatic group of polymer and enzyme, the biosensor could be achieved without using any membrane or covalent bonding between the polymer and enzyme. By using amperometric measurement, cholesterol could be measured at -0.7 V with a LOD and a sensitivity of 0.404 μM and 1.47 mA $mM^{-1}cm^{-2}$, respectively.

For the detection of total cholesterol, cholesterol ester is hydrolyzed by cholesterol esterase (ChEt) to produce free cholesterol for continue reacting with cholesterol oxidase (ChOx) (Figure 2.12). Solanki *et al.* [50] employed the nanobiocomposite of sol-gel-derived silica (SiO_2)/chitosan/MWCNT film deposited onto the ITO glass for the immobilization of ChOx/ChEt. For the detection of cholesterol oleate, this biosensor showed the shelf-life of about 10 weeks, very low value of K_m^{app} as 0.052 mM and a sensitivity of 3.8 μAmM^{-1}.

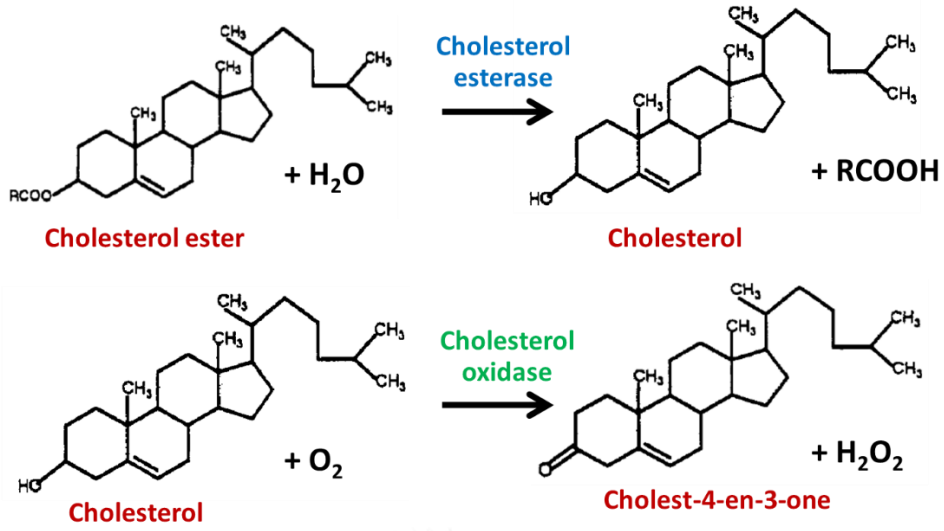

Figure 2.12 Pathway of hydrolysis of cholesterol ester by cholesterol esterase (ChEt) and cholesterol oxidase (ChOx).

2.5.2 Hydrazine

Hydrazine (N_2H_4) is an inorganic agent which is a water-soluble volatile colorless liquid. The structure of hydrazine is showed in Figure 2.13. Hydrazine is extensively used in industrial application, such as reducing agent in fuel cells, corrosion inhibitors, antioxidants and catalysts. Particularly, it is utilized as a starting material in manufacturing of agricultural chemicals, such as pesticides, herbicides, and plant grow regulators [51, 52]. However, hydrazine is an extremely toxic and carcinogenic agent. It is easily adsorbed through oral, skin, inhalation and it cause serious damage to lung, kidney and central nervous system. Therefore, development of an effective method for sensitive detection of hydrazine is greatly required.

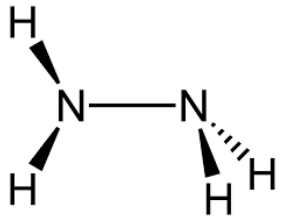

Figure 2.13 Chemical structure of hydrazine.

Conventional analytical methods, such as spectrophotometric method [53, 54], flow injection analysis (FIA) [55, 56], liquid chromatography (LC) [57], gas chromatography-mass spectrometry (GC-MS) [58, 59] have been employed in the determination of hydrazine. Nonetheless, these methods are involved with relative narrow linear range, long analysis time, and expensive instrument, while electrochemical techniques are rapid, simple, portable and inexpensive. The pKa value hydrazine is 8.1 and the oxidation process of hydrazine is expressed as following:

$$N_2H_5^+ \longrightarrow N_2\,(g) + 5H^+ + 4e^- \qquad [41, 60] \qquad (2.9)$$

However, it has been reported that traditional electrochemical system using carbon electrode showed slow electro kinetics of hydrazine oxidation and required large overpotentials [41, 61]. Various modified electrodes have been applied for the hydrazine sensor.

Wang, Y *et. al.* [62] developed a novel polyvinylpyrrolidone-protected silver nanocubes modified glassy carbon electrode (PVP-AgNCs/GCE) for the determination of hydrogen peroxide (H_2O_2) and hydrazine. The developed sensor showed a high sensitivity toward hydrazine oxidation at 0.4 V with a low detection limit of 1.1 μM and a fast response time of less than 2 s.

Kim, S. P. *et. al*. [63] prepared hydrazine sensor using electrode modified with the novel nanocomposite of titanium oxide (TiO_2) nanoparticle deposition on thiolated carbon nanotube (CNT). The average size of TiO_2 nanoparticles on the CNT surface was found to be 4.4 nM. The analytical performances of the prepared hydrazine sensor exhibited a detection limit of 0.22 μM with a linear range of 0.35-162 μM and showed a stable response even in the presence of interferences.

Zhang, C. *et. al.* [41] used gold nanoparticles/zinc oxide-multiwall carbon nanotube modified glassy carbon electrode (AuNPs/ZnO-MWCNT/GCE) as a hydrazine sensor. The developed electrode exhibited a low detection limit of 0.15 μM, a wide linear range and a high sensitivity.

CHAPTER III

EXPERIMENTAL

In this chapter, the details about experiment including chemical and reagent, instrument and equipment, and sample preparation procedure are provided.

3.1 Graphene-Polyvinylpyrrolidone/Polyaniline Nanocomposite Modified Electrode for the Determination of Cholesterol

3.1.1 Chemicals and reagents

- Graphene (G) nanopowders (skyspring Nanomaterials, Inc., Houston, TX)
- Polyaniline (PANI; Mw = 65,000) (Sigma, St. Louis, MO)
- Polyvinylpyrrolidone (PVP; Mw = 10,000) (Sigma, St. Louis, MO)
- Polystyrene (PS; Mw = 180,000) (Sigma, St. Louis, MO)
- Cholesterol oxidase (ChOx) from *Streptomyces sp.* (Sigma, St. Louis, MO)
- Phosphate buffer saline powder (PBS) (Sigma, St. Louis, MO)
- Camphor-10-sulfonic acid (CSA) (Sigma, St. Louis, MO)
- Potassium ferricyanide ($K_3[Fe(CN)_6]$) and potassium ferricyanide ($K_4[Fe(CN)_6]$) (Sigma, St. Louis, MO)
- Dimethylformamide (DMF) (Carlo Erba Reagents, Milano, Italy)
- Chloroform (Carlo Erba Reagents, Milano, Italy)
- Potassium chloride (KCl) (RFCL. Ltd., New Delhi, India)
- Carbon paste and silver/silver chloride paste (Gwent group, Torfaen, United Kingdom).

3.1.2 Instrument and equipment

- Syringe pump (New Era Pumps, NE300, USA)
- High voltage DC module (Gamma High voltage, model UC5-30P/CM/ VM (3), Florida, USA)
- A μAUTOLAB type III potentiostat (Metrohm Siam Company Ltd.)

- Scanning electron microscope (SEM) (JSM-6400; Japan Electron Optics Laboratory Co., Ltd, Japan)
- Transmission electron microscope (TEM) (JEM-2100; Japan Electron Optics Laboratory Co., Ltd, Japan)
- Block screen (Chaiyaboon Co., Bangkok, Thailand)

3.1.3 Preparation of stock solutions for electrochemical detection

All aqueous solutions were prepared by using Milli Q water (12.8 $M\Omega cm^{-1}$)

3.1.3.1 Preparation of 0.1 M phosphate buffer solution (PBS)

1.405 g potassium dihydrogen phosphate (KH_2PO_4) and 2.083 g disodium hydrogen phosphate (Na_2HPO_4) were dissolved in 250 mL of Milli Q water. The prepared solution pH was adjusted to a pH of 7.0 by using 0.1 M sodium hydroxide or 0.1 M hydrochloric acid. 0.1 M PBS solution was used as a supporting electrolyte for cholesterol and hydrazine detection.

3.1.3.2 Preparation of 0.5 M potassium chloride (KCl)

0.5 mM KCl was prepared by dissolving 9.31 g KCl in 250 mL of Milli Q water.

3.1.3.3 Preparation of 5 mM Ferri/ferrocyanide $[Fe(CN)_6]^{3-/4-}$

5 mM $[Fe(CN)_6]^{3-/4-}$ was prepared by dissolving 0.1646 g Ferricyanide $[Fe(CN)_6]^{3-}$ and 0.2112 g Ferricyanide $[Fe(CN)_6]^{4-}$ in 100 mL of 0.5 M KCl. The stock solution of $[Fe(CN)_6]^{3-/4-}$ was further diluted to make different concentrations in 0.5 M KCl.

3.1.3.4 Preparation of 1 mM hydrogen peroxide (H_2O_2)

1 mM H_2O_2 was prepared by dilution of 30% H_2O_2 standard solution 2 µL in 998 µL of 0.1 M PBS (pH 7.0).

3.1.3.5 Preparation of stock standard solution of cholesterol

10 mM cholesterol solution was prepared by dissolving cholesterol (3.86 mg) in 70 mg of (5 % w/v) Triton-X. The resulting solution was gently heated and stirred to obtain a clear solution. Then, 1 mL of 0.1 M PBS (pH 7.0) was added and stored

at 4 °C. The stock solution of cholesterol was further diluted to make different concentrations in 0.1 M PBS (pH 7.0).

3.1.3.6 Preparation of cholesterol oxidase enzyme (ChOx)

39 units mL^{-1} ChOx solution was prepared by dissolving 1 mg of ChOx in 1 mL of PBS (0.1 M, pH 7.0).

3.1.4 Preparation of screen-printed carbon electrode (SPCE)

The three-electrodes were prepared via screen-printed fabrication on polyvinylchloride (PVC) substrate using a block screen. Firstly, reference electrode (RE) and conductor was screen-printed on PVC substrate using silver/silver chloride (Ag/AgCl) paste and heated up at 50 °C for 1 h in an oven. After that, carbon paste was screen-printed as a working electrode (WE) and a counter electrode (CE) and heated up again at 50 °C for 1 h. Finally, the SPCEs were obtained with the WE surface area of 0.126 cm^2. A pattern of SPCEs used in this study was shown in Figure 3.1.

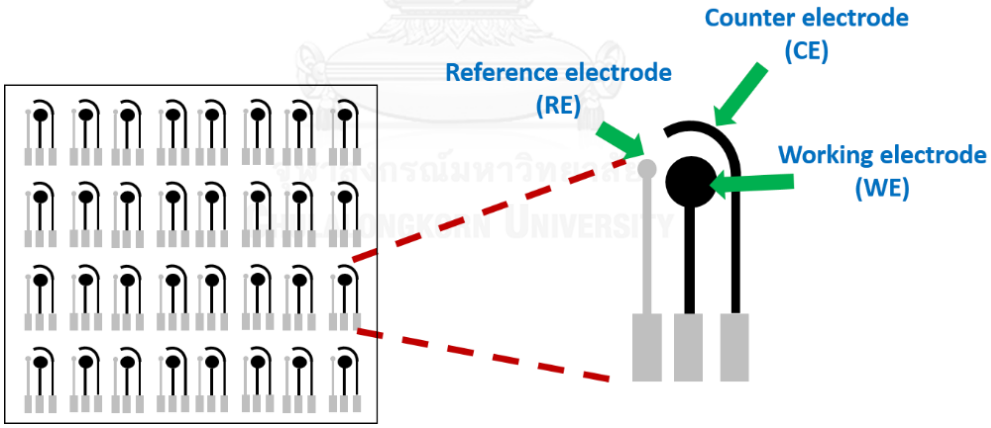

Figure 3.1 The three-electrode system of SPCE used in this study.

3.1.5 Modification of screen-printed carbon electrode (SPCE)

3.1.5.1 Preparation of G-PVP/PANI nanocomposite solution

To prepare G-PVP/PANI nanocomposite solution, G (0.02 g) were dispersed in 5 mL of DMF containing PVP (0.02 g) as a stabilizer and sonicated for 12 h at a room temperature. PANI (0.4 g) and CSA (0.516 g) were dissolved in 15 mL of chloroform

and then stirred by mechanical stirrer for 12 h. After that, the PANI solution was filtered through a filter paper to remove the particles. Then, G-PVP and PANI solution were mixed together (ratio 1:1), and added with 0.1% (v/v) PS [39].

3.1.5.2 Electrospraying fabrication

For electrode surface modification, the mixed G-PVP/PANI solution was modified on working electrode (WE) by using electrospraying fabrication. Prior to modification, WE and CE were covered with mask and then the three-electrodes were attached to the ground collector. The nanocomposite solution was placed in a syringe and electrosprayed using an in-house electrospraying system as shown in Figure 3.2. In electrospraying process, all parameters were optimized. The applied voltage was 6 kV, the flow rate of the solution was 1 mL hr^{-1}, and the distance between needle tip and ground collector was 5 cm, respectively. When a high voltage was applied, G-PVP/PANI solution in a syringe was electrosprayed as small droplets from the needle tip onto the WE surface attached on a ground collector.

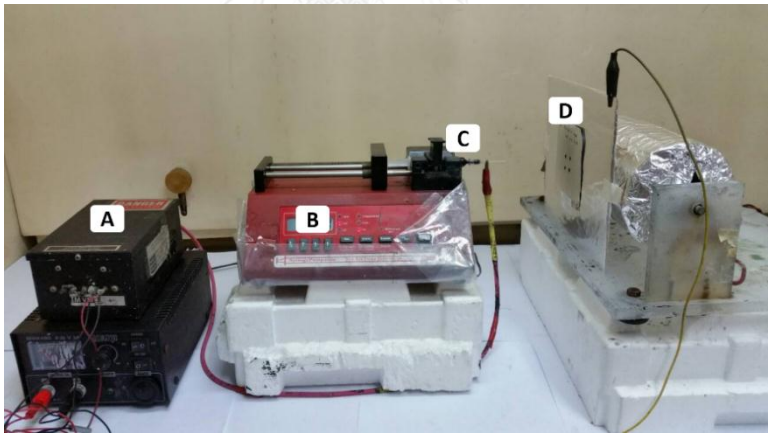

Figure 3.2 An in-house electrospraying; (A) high power supply, (B) syringe pump, (C) a syringe containing G-PVP/PANI solution and (D) SPCE attached on a ground collector.

3.1.5.3 Optimization of electrode modification

%G loading was varied from 0.025 to 0.4 % w/v and %PANI loading was varied from 0.17 to 1.36 % w/v. To optimize %G and %PANI loading, cyclic voltammetry (CV) of standard $[Fe(CN)_6]^{3-/4-}$ redox couple was carried out.

3.1.5.4 Immobilization of cholesterol oxidase (ChOx) on G-PVP/PANI modified SPCE

After optimization of electrode modification, optimal condition of the %G and %PANI loading in previous experiment (section 3.1.5.3) was used in immobilization step. ChOx was immobilized onto G-PVP/PANI modified SPCE by covalent linkage using glutaraldehyde as a crosslinking agent. First, the 5 µL of 0.1% (v/v) glutaraldehyde was dropped on G-PVP/PANI modified SPCE and allowed to dry. After that, the 5 µL of ChOx solution was added and kept overnight at 4 °C. Finally, the G-PVP/PANI modified SPCE was washed 3 times with PBS (0.1 M, pH 7.0) to remove un-bound or loosely bound enzyme molecules and stored at 4 °C until it was used.

3.1.6 Characterization of modified electrode

3.1.6.1 Surface morphology characterization

The surface morphology of the G-PVP/PANI nanocomposite modified SPCE was characterized using scanning electron microscopy (SEM). The dispersion of G-PVP/PANI nanocomposite on the modified electrode surface was characterized using transmission electron microscopy (TEM).

3.1.6.2 Electrochemical characterization

For all electrochemical measurements including cyclic voltammetry, amperometry and electrochemical impedance spectroscopy, a µAUTOLAB type III potentiostat was employed with the fabricated three-electrode system.

For optimization of %G and %PANI loading, cyclic voltammetric measurement (CV) of standard ferri/ferrocyanide $[Fe(CN)_6]^{3-/4-}$ was employed in a range of -0.5 to +1.0 V. Then, optimal conditions was used for hydrogen peroxide (H_2O_2) and cholesterol detection by amperometric measurement at 0.6 V and recorded the steady state current at 100 s.

3.2 Nitrogen-Doped Graphene-Polyvinylpyrrolidone/Gold Nanoparticles Modified Electrode as a Novel Hydrazine Sensor

3.2.1 Chemicals and reagents

- Nitrogen doped graphene (NG) nanopowders (XF Nano,Inc, Nanjing, China)
- Polyvinylpyrrolidone (PVP; Mw = 10,000) (Sigma, St. Louis, MO)
- Polystyrene (PS; Mw = 180,000) (Sigma, St. Louis, MO)
- Gold (III) chloride solution ($HAuCl_4$) (Sigma, St. Louis, MO)

3.2.2 Instrument and equipment

- Syringe pump (New Era Pumps, NE300, USA)
- High voltage DC module (Gamma High voltage, model UC5-30P/CM/ VM (3), Florida, USA)
- A μAUTOLAB type III potentiostat (Metrohm Siam Company Ltd.)
- CHI 1240B electrochemical analyzer (CH Instruments, Inc., USA)

3.2.3 Preparation of stock solutions for electrochemical detection

All aqueous solutions were prepared by using Milli Q water (12.8 $M\Omega cm^{-1}$)

3.2.3.1 Preparation of 0.5 M sulfuric acid solution (H_2SO_4)

0.5 M H_2SO_4 solution was prepared by diluting 2.776 mL of 96% w/w concentrated H_2SO_4 to 100 mL with Milli Q water.

3.2.3.2 Preparation of stock solution of gold (III) chloride ($HAuCl_4$)

10 mM $HAuCl_4$ solution was prepared by diluting 0.0692 mL of 30% w/v (1.445M) $HAuCl_4$ solution to 10 mL with 0.5 M H_2SO_4.

3.2.3.3 Preparation of stock solution of hydrazine

20 mM hydrazine was freshly prepared by dissolving 7.8 mg of hydrazine sulfate in 3 mL of 0.1 M PBS (pH 7.0). The stock solution of hydrazine was further diluted to make different concentrations in 0.1 M PBS (pH 7.0).

3.2.4 Modification of screen-printed carbon electrode (SPCE)

3.2.4.1 Electrospraying of NG-PVP nanocomposite on SPCE

To prepare NG-PVP nanocomposite solution, 1 mg of NG powders were dispersed in 1 mL of DMF containing 0.5 mg mL^{-1} PVP as a stabilizer and sonicated for 4 h at a room temperature. After that, NG-PVP solution was mixed with 0.15 % (w/v) PS in chloroform and then modified on the working electrode (WE) using an in-house electrospraying fabrication. After optimization, an applied voltage on the needle tip was 4.5 kV, the flow rate of the solution through the needle tip was kept steady by a syringe pump at 2 mL hr^{-1}, and the distance between needle tip and ground collector was 5 cm.

3.2.4.2 Electrochemical deposition of AuNPs on NG-PVP modified electrode

The 100 uL of 1 mM $HAuCl_4$ in 0.5 M H_2SO_4 was dropped on the NG-PVP modified SPCE. After that, CV scanning from -0.5 to 1 V (vs. Ag/AgCl) at 50 mV s^{-1} for 3 cycles was carried out. Eventually, AuNPs were electrochemically deposited on NG-PVP modified SPCE to provide NG-PVP/AuNPs modified SPCE.

3.2.5 Optimization of SPCE modification

Three main parameters for SPCE modification composition (*i.e.* NG loading, $HAuCl_4$ concentration and number of cycles for AuNPs electrodeposition) were optimized to obtain the highest current response for hydrazine. The optimization of SPCE modification was investigated by measuring CV current response of 0.1 mM hydrazine in 0.1 M PBS, pH 7.0.

3.2.5.1 Effect of NG loading

The effect of NG loading was investigated by dispersing 0.5, 1.0, 1.5, 2.0 and 2.5 mg of NG in 1.0 mL of DMF containing 0.5 mg of PVP and sonicating for 4 h. After that, the prepared NG-PVP solution was electrosprayed on SPCE surface.

3.2.5.2 Effect of $HAuCl_4$ concentration

The effect of $HAuCl_4$ concentration was investigated by using different concentrations of $HAuCl_4$ including 0.5, 1.0, 3.0, 5.0 and 7.0 mM in electrodeposition of AuNPs.

3.2.5.3 Effect of number of cycles for AuNPs electrodeposition

The effect of number of cycles was investigated by using different cycles for AuNPs electrodeposition including 1, 3, 5, 7 and 9 cycles.

3.2.6 Optimization of parameters in square wave voltammetric measurement (SWV parameters)

The optimization of SWV parameters was investigated by measuring the SWV response of 50 μM hydrazine in 0.1 M PBS (pH 7.0). The step potential in the range from 4–20 mV, the amplitude in the range of 20–120 mV and the frequency in the range from 5–30 Hz were studied.

3.2.7 Characterization of modified electrode

3.2.7.1 Surface morphology characterization

The surface morphology of unmodified SPCE, NG-PVP modified SPCE and NG-PVP/AuNPs modified SPCE were characterized by scanning electron microscopy (SEM). Moreover, transmission electron microscopy (TEM) was used for investigation of NG-PVP nanocomposites dispersion.

3.2.7.2 Electrochemical characterization

For the electrochemical measurements including cyclic voltammetry (CV) and square wave voltammetry (SWV), a CHI 1240B electrochemical analyzer was employed. The electrochemical behavior of modified SPCE was investigated by CV of hydrazine in 0.1 M PBS (pH 7.0) over a potential range of -0.5 to +0.5 V and a scan rate of 100 mV s^{-1}. SWV measurements of hydrazine were carried on an applied potential from -0.5 to +0.5 V with the optimal parameters.

Furthermore, electrochemical impedance spectroscopy (EIS) was performed on a μAUTOLAB type III potentiostat using a solution of 0.5 M KCl containing 1 mM $[Fe(CN)_6]^{3-/4-}$ with the frequency range from 0.1 to 10^{-5} Hz and an amplitude of 0.01 V. The set-up of electrochemical system used in this study is shown in the Figure 3.3.

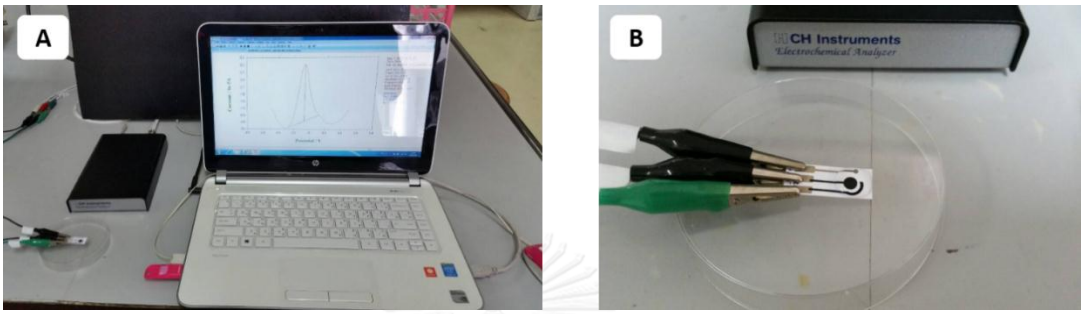

Figure 3.3 (A) The set-up of full electrochemical system and (B) the SPCE used in the electrochemical system.

3.2.8 The analytical performances of NG-PVP/AuNPs modified SPCE

The investigation of analytical performances was performed on SWV measurement.

3.2.8.1 Calibration plot

20 mM hydrazine stock solution was diluted to different concentrations and then employed for SWV measurement using NG-PVP/AuNPs modified SPCE. After that, the linear relationship between concentration of hydrazine and anodic current response was plotted to obtain a linear range of the system.

3.2.8.2 Limit of detection (LOD)

The limit of detection (LOD) was calculated using the formula of $LOD = 3S_b/m$, where S_b is a standard deviation of a signal obtained from a blank solution (seven-time determinations), m is a slope of calibration curve.

3.2.8.3 Repeatability and reproducibility

The SWV measurement of 50 µM hydrazine was employed for investigation of repeatability and reproducibility. For repeatability, the same modified SPCE was used for ten successive scans. The reproducibility was investigated by measuring the hydrazine concentration on five independent modified SPCE. The percentage of relative standard deviation (%RSD) was calculated by using a shown equation below:

$$\%\,\mathbf{RSD} = \frac{\mathbf{Standard\ daviation}}{\mathbf{Mean}} \times \mathbf{100} \qquad (3.1)$$

3.2.8.4 Interference study

The 50 mM stock solutions of potential interferences including K^{+}, Na^{+}, Mg^{2+}, Ca^{2+}, Zn^{2+}, Fe^{3+}, NO^{3-}, SO_4^{2-}, glucose, sucrose and lactose was prepared. The selectivity of modified SPCE was evaluated by measuring of 50 µM hydrazine in the presence of different interferences. In this study, the tolerance limit is defined as the molar ratio of potential interferences/hydrazine that caused the ±5% change in the current response of hydrazine.

3.2.9 Real sample analysis

3.2.9.1 Real sample preparation

The real samples in this study consisted of sapodilla, sweet corn and sugarcane. Sapodilla and sweet corn were purchased as raw products while sugarcane was purchased as freshly squeezed sugarcane juice from local super market in Thailand. For sapodilla, its skin was cleaned in running tap water, left to dry and then its unseeded flesh was sliced into small pieces. For sweet corn, its husk was removed and its kernels were knifed off from its core. Next, the slides of each sample (*i.e.* sapodilla and sweet corn) were blended together using electronic blender and filtered through nylon mesh (pore size = 70 µm). Next, the filtered juices were centrifuged at 16,000 rpm for 30 min and the supernatants were collected. After that, the sugarcane and sapodilla juice were diluted for 20 times while sweet corn juice was diluted for 100 times with 0.1 M PBS (pH 7.0). Finally, the hydrazine standard solutions were spiked in the as prepared juices by standard addition with the final concentrations of 10, 50 and 100 µM prior to analysis.

3.2.9.2 Recovery

In real sample analysis, the percentage of recovery was employed to evaluate the applicability of the purposed system by using a standard addition method. The % recovery was calculated using the following equation:

$$\%\ \mathbf{Recovery} = \frac{\mathbf{Measured\ value\ of\ spiked\ sample} - \mathbf{Measured\ value\ of\ unspiked\ sample}}{\mathbf{Known\ value\ of\ spiked\ sample}} \times \mathbf{100}$$

CHAPTER IV
RESULTS AND DISCUSSION

In this chapter, the results including optimization of electrode modification, surface morphology characterization, electrochemical characterization and determination of target analytes are discussed.

4.1 Graphene-Polyvinylpyrrolidone/Polyaniline Nanocomposite Modified Electrode for the Determination of Cholesterol

4.1.1 The optimization of SPCE modification

Prior to immobilization of ChOx for cholesterol determination, the factors affecting the electrochemical performances of the modified SPCE including applied voltage of electrospraying and the percentage of G and PANI loading (%G and %PANI) were evaluated and optimized. Among all, %G and %PANI loadings were the crucial factors affecting the electrochemical sensitivity of modified SPCE. To optimize %G and %PANI loading, cyclic voltammetric measurements (CV) of standard $[Fe(CN)_6]^{3-/4-}$ redox couple were carried out.

4.1.1.1 Effect of G loading

To study the effect of %G loading, the electrodes were modified with G-PVP/PANI nanocomposite using different %G in a range of 0.025 to 0.4% (w/v). As shown in Figure 4.1, the integrated anodic currents of modified SPCE increased when %G increased from 0.025 to 0.1%, verifying that G can enhance the electrochemical sensitivity of the system. However, the current response decreased when %G increased in a range from 0.2 to 0.4%. The decrease in current response was probably caused by agglomeration of G at high concentration leading to the decreased electrochemical response. Moreover, due to miniscule amount of G used in this study, the preparation of 0.1% G was more practical than 0.025% G for weighing purpose. Thus, an optimal condition of G loading was 0.1% (w/v) and this condition will be used for further studies.

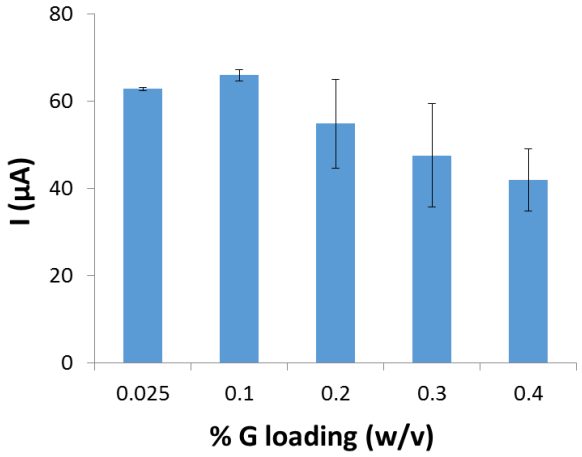

Figure 4.1 The effect of %G loading on the anodic peak current (I_{pa}) in CVs of 1 mM standard $[Fe(CN)_6]^{3-/4-}$ in 0.5 M KCl using G-PVP/PANI modified SPCE.

4.1.1.2 Effect of PANI loading

The %PANI loading was studied in a range of 0.17 to 1.36% (w/v) as shown in Figure 4.2. The results showed that the increase of PANI loading in a range from 0.17 to 1.36% can increase the current responses of $[Fe(CN)_6]^{3-/4-}$. The modified SPCE showed the highest current responses at 1.36% PANI loading, indicating the highest electrochemical sensitivity. Furthermore, using more than 1.36 % PANI was limited by its solubility at higher concentration, therefore, 1.36% (w/v) PANI loading was selected for all further experiments.

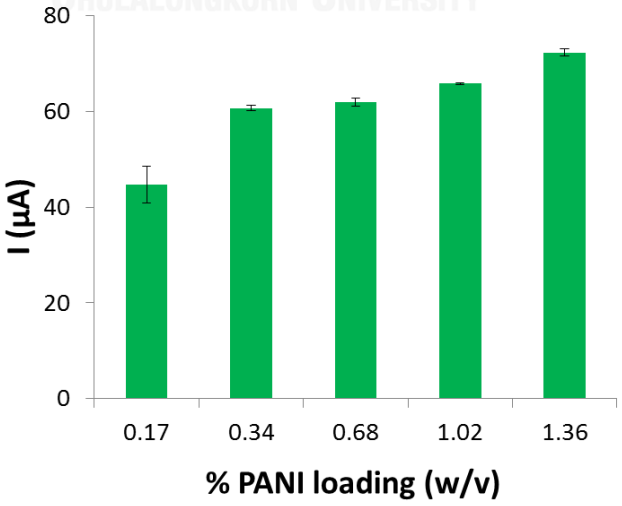

Figure 4.2 The effect of %PANI loading on the anodic peak current (I_{pa}) in CVs of 1 mM standard $[Fe(CN)_6]^{3-/4-}$ in 0.5 M KCl using G-PVP/PANI modified SPCE.

4.1.2 Characterization of G-PVP/PANI modified SPCE

4.1.2.1 Surface morphology characterization

After optimization of electrode modification, the morphology and dispersion of G-PVP/PANI nanocomposites were characterized by scanning electron microscopy (SEM) and transmission electron microscopy (TEM), respectively. As shown in Figure 4.3A, an SEM image showed the uniform 3D droplet-like nanostructures of G-PVP/PANI with an average droplet size of 180 ± 29 nm. Moreover, a TEM image of the nanocomposite (Figure 4.3B), as well as electron diffraction pattern of G (inset of Figure 4.3B), revealed that G was well dispersed within the matrix of nanocomposite without any severe agglomeration.

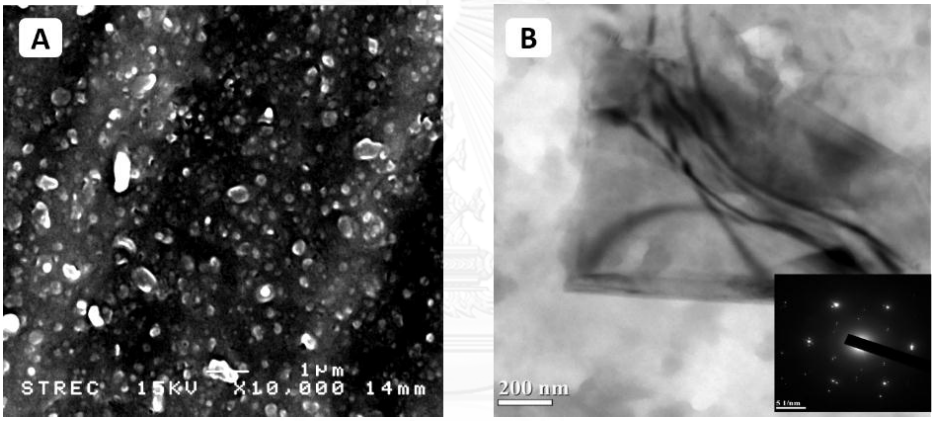

Figure 4.3 (A) an SEM image of G-PVP/PANI modified SPCE. (B) A TEM image of G-PVP/PANI nanocomposite and electron diffraction pattern of G dispersed in the nanocomposites (inset of B).

4.1.2.2 Electrochemical characterization

Other than the surface morphology characterization, the electrochemical performance of G-PVP/PANI modified SPCE was investigated by cyclic voltammetry of 1 mM standard $[Fe(CN)_6]^{3-/4-}$, compared with unmodified SPCE and PANI modified SPCE as shown in Figure 4.4. It could be seen that the anodic and cathodic peak currents increased from unmodified SPCE (yellow), PANI modified SPCE (green) and G-PVP/PANI modified SPCE (red), respectively. The highest current response obtained from G-PVP/PANI modified SPCE (red) indicated that G-PVP/PANI nanocomposite can

substantially increase the electrochemical sensitivity of the modified SPCE. Furthermore, the peak-to-peak potential separation (ΔEp) of G-PVP/PANI modified SPCE (ΔEp = 0.300; red) was significantly decreased compared to unmodified SPCE (ΔEp = 0.647; yellow) and PANI modified SPCE (ΔEp = 0.571; green) indicating the faster rate of electron transfer kinetic of G-PVP/PANI modified SPCE.

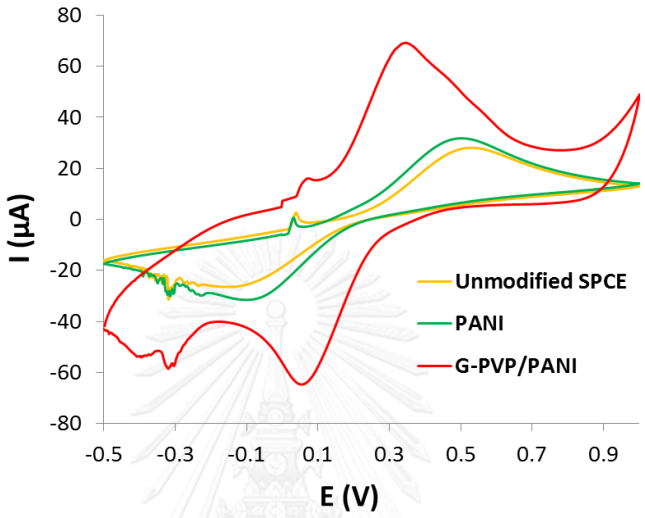

Figure 4.4 CVs of 1 mM standard $[Fe(CN)_6]^{3-/4-}$ in 0.5 M KCl measured on unmodified SPCE (yellow), PANI modified SPCE (green) and G-PVP/PANI modified SPCE (red).

4.1.3 Hydrogen peroxide (H_2O_2) and cholesterol determination

The electrochemical properties of G-PVP/PANI modified SPCE towards H_2O_2 were studied by amperometric measurement as shown in Figure 4.5. The G-PVP/PANI modified SPCE showed 46-fold higher in current responses toward 1 mM H_2O_2 compared to an unmodified SPCE, indicating that the modified SPCE could be potentially applied for cholesterol determination through the detection of H_2O_2 (by-product of cholesterol oxidation). The biochemical reaction of cholesterol involved in electrochemical detection of H_2O_2 was shown as the followings:

$$\text{Cholesterol} + O_2 \xrightarrow{\text{ChOx}} \text{Cholest-4-en-3-one} + H_2O_2 \quad [64] \quad (4.1)$$

$$H_2O_2 \longrightarrow 2H^+ + O_2 + 2e^- \quad (4.2)$$

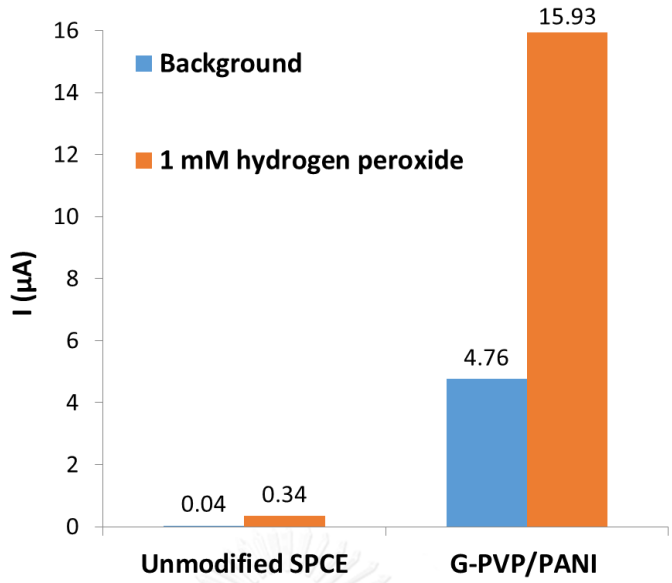

Figure 4.5 The amperometric current responses of 1 mM H_2O_2 and background in PBS (0.1 M, pH 7.0) measured at 0.6 V using unmodified SPCE and G-PVP/PANI modified SPCE.

For enzymatic determination of cholesterol, cholesterol oxidase (ChOx) was covalently immobilized onto G-PVP/PANI modified SPCE to obtain the ChOx/G-PVP/PANI modified SPCE. In addition, the large surface area of G-PVP/PANI nanodroplets was very useful for further enzyme loading. As shown in Figure 4.6, the ChOx/G-PVP/PANI modified SPCE exhibited the highest current responses for amperometric determination of cholesterol, which was 3-time higher than G-PVP/PANI modified SPCE and 18-time greater than unmodified SPCE. Thus, the immobilization of ChOx onto G-PVP/PANI modified SPCE resulted in substantially improved sensitivity for cholesterol.

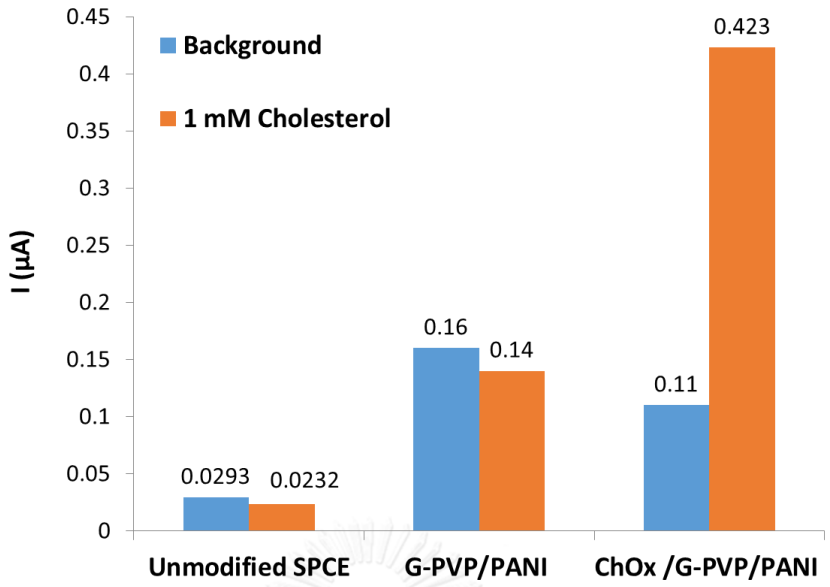

Figure 4.6 The amperometric current responses of 1 mM cholesterol and background in PBS (0.1 M, pH 7.0) measured at 0.6 V using different electrodes.

Since the previous work of our research group, Ruecha *et. al.* [39], on development of the disposable cholesterol biosensor based on ChOx/G-PVP/PANI using paper as substrate was already accomplished. The objective of this study is to make the improvement of this previous work in 2 areas: a) to develop the total cholesterol biosensor based on the immobilization of cholesterol oxidase (ChOx) and cholesterol esterase (ChEt), and b) to improve the reusability of the cholesterol biosensor.

The sequence of enzymatic reactions was described below:

$$\text{Cholesterol ester} + H_2O \xrightarrow{\text{ChEt}} \text{Free cholesterol} + \text{Fatty acid} \qquad (4.3)$$

$$\text{Free cholesterol} + O_2 \xrightarrow{\text{ChOx}} \text{Cholest-4-en-3-one} + H_2O_2 \quad [64] \qquad (4.4)$$

However, after the chemical immobilization of ChEt and ChOx on the G-PVP/PANI modified SPCE, the current response of cholesterol ester measured on ChEt-ChOx/G-PVP/PANI modified SPCE did not show any change from the background current which was probably cause by the problem in converting cholesterol ester to free cholesterol.

Furthermore, in this thesis, the PVC sheet was used as a substrate to improve the reusability of the cholesterol biosensor. However, due to the lower surface area of PVC substrate, the ChOx/G-PVP/PANI biosensor on PVC substrate showed the lower sensitivity for the detection of free cholesterol compared to Ruecha's work. Although the researcher had tried to overcome these limitations using different strategic approaches, we still could not achieve desirable results. Therefore, the objective of this study was changed by focusing on different target analytes instead of cholesterol.

Next, hydrazine was selected as a target analyte in this study because it is extremely toxic and carcinogenic, which can cause the serious effects on human health. Initially, the detection of hydrazine was based on the use of G-PVP/PANI modified SPCE, but this modified SPCE still showed low sensitivity; therefore, the system is needed to be improved. After the intensive studies, the researcher found that the use of the nitrogen-doped graphene (NG) showed 3-time increase in anodic current of hydrazine compared to the use of G. Furthermore, AuNPs have been used as an electrocatalytic electrode for hydrazine detection, thus this study will focus on using NG-PVP along with AuNPs in the detection of hydrazine to obtain the highest system performance.

4.2 Nitrogen-Doped Graphene-Polyvinylpyrrolidone/Gold Nanoparticles Modified Electrode as a Novel Hydrazine Sensor

For SPCE surface modification, two modification steps including electrospraying of NG-PVP and electrodeposition of AuNPs were used to fabricate NG-PVP/AuNPs modified SPCE. To generate NG-PVP nanocomposite on SPCE surface, electrospraying was selected to increase a surface area of the modified SPCE. Moreover, polystyrene (PS) used as carrier polymer to facilitate the electrospraying was mixed with NG-PVP prior to electrospraying. After electrospraying of NG-PVP, AuNPs were electrochemically deposited onto NG-PVP modified SPCE.

4.2.1 Optimization of SPCE modification

For electrode surface modification, the factors affecting the analytical performances of NG-PVP/AuNPs modified SPCE were evaluated and optimized using cyclic voltammetry (CV) of hydrazine. Among all parameters, the amount of NG loading, concentration of $HAuCl_4$ solution and a number of cycles for AuNPs electrodeposition were the key factors showing a profound impact on an electrochemical detection of hydrazine.

4.2.1.1 Effect of NG loading

Initially, the amount of NG loading was varied in a range from 0.5 to 2.5 mg mL^{-1} as shown in Figure. 4.7. It was found that the anodic current response increased when the amount of NG loading increased from 0.5 to 1.0 mg mL^{-1}, indicating that adding more NG in the nanocomposites can enhance the electrochemical sensitivity of modified SPCE. After that, the anodic peak currents gradually decreased when the amount of NG loading decreased in a range of 1.0 to 2.5 mg mL^{-1}. This decrease is probably caused by the self-agglomeration of NG at the high concentration, leading to decreased surface area of NG and resulting in the decreased electrochemical responses. Thus, 1.0 mg mL^{-1} of NG loading was used for further experiments.

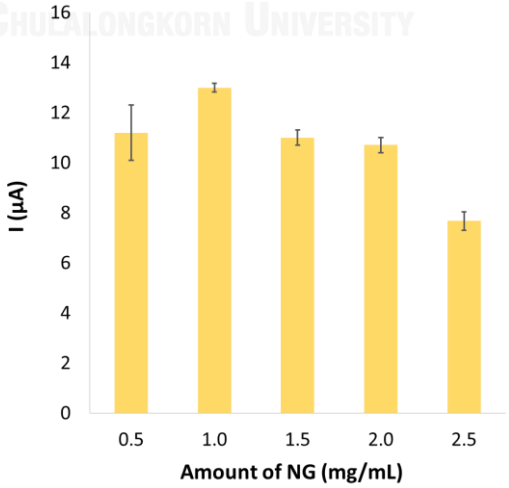

Figure 4.7 The effect of amount of NG loading on the anodic peak current (I_{pa}) obtained from cyclic voltammograms of 0.1 mM hydrazine in 0.1 M PBS (pH 7.0) measured on NG-PVP/AuNPs modified SPCE.

4.2.1.2 Effect of $HAuCl_4$ concentration

Next, the effect of $HAuCl_4$ concentration used in AuNPs electrodeposition onto NG-PVP modified SPCE was investigated. As seen in the Figure 4.8, the anodic peak current increased with the increase of $HAuCl_4$ concentration and the highest peak current was obtained at 1.0 mM of $HAuCl_4$. However, when the concentration of $HAuCl_4$ was higher than 1.0 mM, the anodic peak current response was substantially decreased. This may attribute to the change of AuNPs coating morphology on the NG-PVP modified SPCE with a denser packing of AuNPs into an Au bulk-liked layer instead of AuNPs form leading to a decrease in effective surface area and then resulting in the decreased electrochemical responses. Thus, the further experiments were performed by using 1.0 mM of $HAuCl_4$.

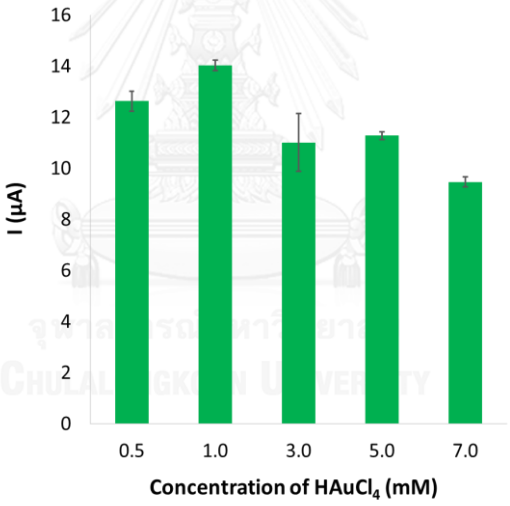

Figure 4.8 The effect of $HAuCl_4$ concentration on the anodic peak current (I_{pa}) obtained from cyclic voltammograms of 0.1 mM hydrazine in 0.1 M PBS (pH 7.0) measured on NG-PVP/AuNPs modified SPCE.

4.2.1.3 Effect of a number of cycles for AuNPs electrodeposition

An effect of a number of cycles for AuNPs electrodeposition was also studied (Figure 4.9). The highest current response was achieved at 3 cycles of AuNPs electrodeposition for the detection of hydrazine. Thus, 3 cycles for AuNPs electrodeposition was used in all further studies.

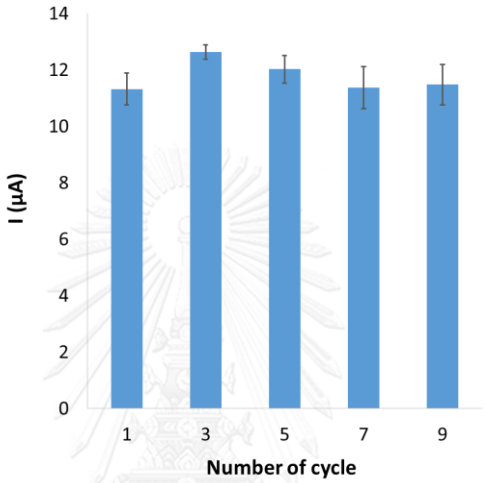

Figure 4.9 The effect of a number of cycles for AuNPs electrodeposition on the anodic peak current (I_{pa}) obtained from cyclic voltammograms of 0.1 mM hydrazine in 0.1 M PBS (pH 7.0) measured on NG-PVP/AuNPs modified SPCE.

4.2.2 Characterization of NG-PVP/AuNPs modified SPCE

4.2.2.1 Surface morphology characterization

At the optimal conditions of modified SPCE, the surface morphology of unmodified SPCE, NG-PVP modified SPCE and NG-PVP/AuNPs modified SPCE was characterized by SEM as shown in the Figure 4.10A, 4.10B and 4.10C, respectively. After electrospraying of NG-PVP, the electrosprayed layers (Figure. 4.10B) consisted of micro and nanoscopic droplets and structures of irregular shape that appeared to fuse together throughout the coating. Large plate-liked structures, presumed to be NG sheets, were also found occasionally on the top most surface of coating. With longer electrospraying time, these droplets built up on top of the previous electrosprayed layers resulting in a 3 dimension-liked coating with shallow hill-and-

valley geometry, leading to substantially increased electrode surface area. After that, the electrosprayed NG-PVP nanocomposite layer was decorated uniformly with electrochemically deposited AuNPs (Figure. 4.10C). The results from energy dispersive X-ray spectroscopy (EDX) measurement (Figure 4.10D) showed that the weight content of C, O, Cl, Au, is 85.57%, 8.51%. 1.14%, 4.78%, respectively and the atom content of C, O, Cl, Au, is 92.37%, 6.90%, 0.42%, 0.31%, respectively, confirming that the AuNPs were successfully electrodeposited on NG-PVP modified SPCE. The presence of characteristic Cl peaks attributed to the Cl atoms in the PVC substrate of electrode. Furthermore, the dispersion of NG-PVP nanocomposites was also investigated by TEM. A TEM image (Figure 4.10E) revealed that NG was well dispersed within the nanocomposites and the electron diffraction pattern of NG as shown in Figure 4.10F. This pattern was well matched with previous study [11], confirming that NG was randomly dispersed without any severe agglomeration. The modification of SPCE with good dispersion of nanocomposites leaded to increased surface area of SPCE and thereby potentially resulting in enhanced electrochemical sensitivity of the electrochemical sensor.

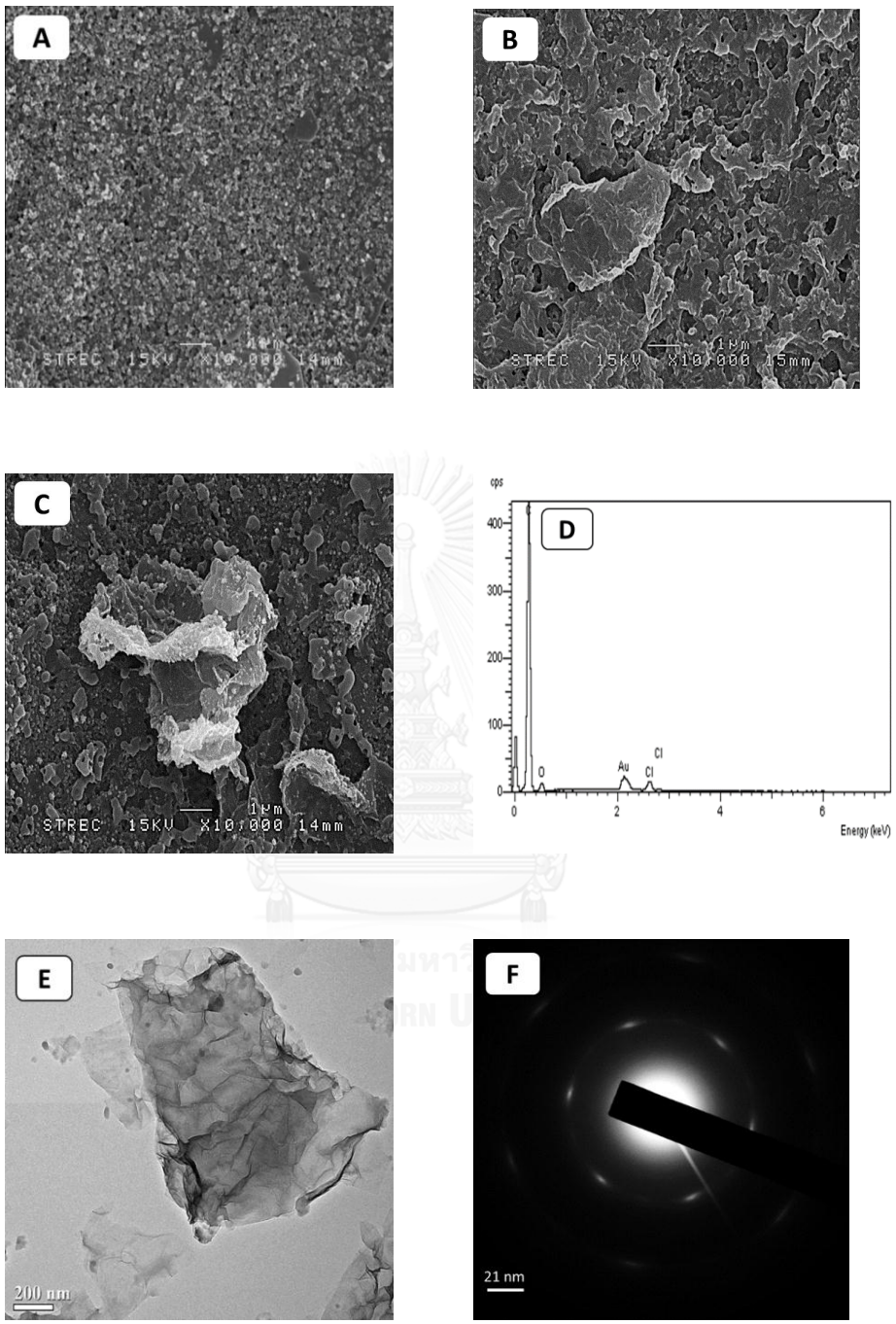

Figure 4.10 SEM images of unmodified SPCE (A), NG-PVP modified SPCE (B), NG-PVP/AuNPs modified SPCE (C); EDX spectra of NG-PVP/AuNPs modified SPCE (D); TEM image of NG-PVP nanocomposite (E); an electron diffraction pattern of NG (F).

4.2.2.2 Electrochemical characterization

To characterize the interfacial properties of modified SPCE, electrochemical impedance spectroscopy (EIS) was used in this study. The magnitude of the electron transfer resistance (R_{ct}) depends on the dielectric and insulating features at the electrode-electrolyte interface. Figure 4.11 showed the Nyquist plots of 1.0 mM $[Fe(CN)_6]^{3-/4-}$ in 0.5 M KCl measured for each step of SPCE modification. The value of R_{ct} derived from a diameter of semicircle of each Nyquist plot is related to the charge transfer resistance and electronic resistance of the electrode. As seen in Figure 4.11, the values of R_{ct} of the electrodes were obtained as 30590 Ω for unmodified SPCE (a), 16260 Ω for NG-PVP modified SPCE (b) and 2572 Ω for NG-PVP/AuNPs modified SPCE (c). Compared to unmodified SPCE, R_{ct} value obtained from NG-PVP modified SPCE decreased to 16260 Ω which indicated that NG-PVP nanocomposite can effectively accelerate the electron transfer of NG-PVP modified SPCE and then resulting in the lower R_{ct} value. After electrodeposition of AuNPs, NG-PVP/AuNPs modified SPCE showed the lowest R_{ct} value. This probably attributed to the high electrical conductivity of AuNPs. Thus, these results verify that NG-PVP/AuNPs nanocomposite can substantially improve the interfacial charge transfer of NG-PVP/AuNPs modified SPCE.

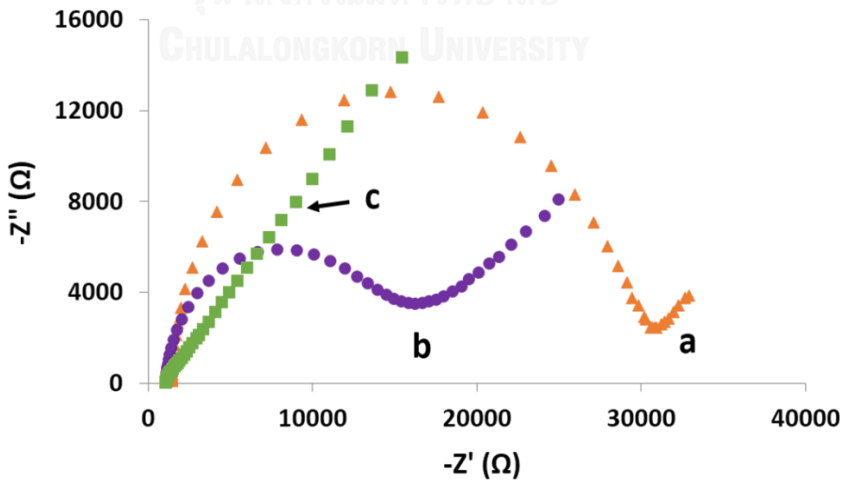

Figure 4.11 EIS of the unmodified SPCE (a), NG-PVP modified SPCE (b) and NG-PVP/AuNPs modified SPCE (c) in the presence of 1.0 mM of $Fe(CN)_6^{3-/4-}$ with 0.5 M KCl.

To investigate the electrochemical behavior of hydrazine oxidation on NG-PVP/AuNPs modified SPCE, cyclic voltammetry (CV) was applied at different scan rates in a range of 5-100 mV s^{-1}, as seen in the Figure 4.12, the anodic peak current (I_{pa}) of hydrazine increased with the increase of scan rate. The relationship between square root of scan rate ($\mathbf{V}^{1/2}$) and anodic peak current showed a linear regression of I_{pa} (μA) = 1.2344 $\mathbf{V}^{1/2}$ $((V\ s^{-1})^{1/2})$ + 0.2638 with a correlation coefficient (R^2) of 0.9975. This linear relationship verifies that the oxidation process of hydrazine on NG-PVP/AuNPs modified SPCE is a diffusion controlled process.

The mechanism of hydrazine oxidation has been studied on different electrodes. The electro-oxidation of hydrazine was mainly involved with four electrons, which releases the N_2 gas as a final product. The overall oxidation mechanism of hydrazine can be described as a following process:

$$N_2H_5^+ \longrightarrow N_2\,(g) + 5H^+ + 4e^- \quad [41, 60] \qquad (4.5)$$

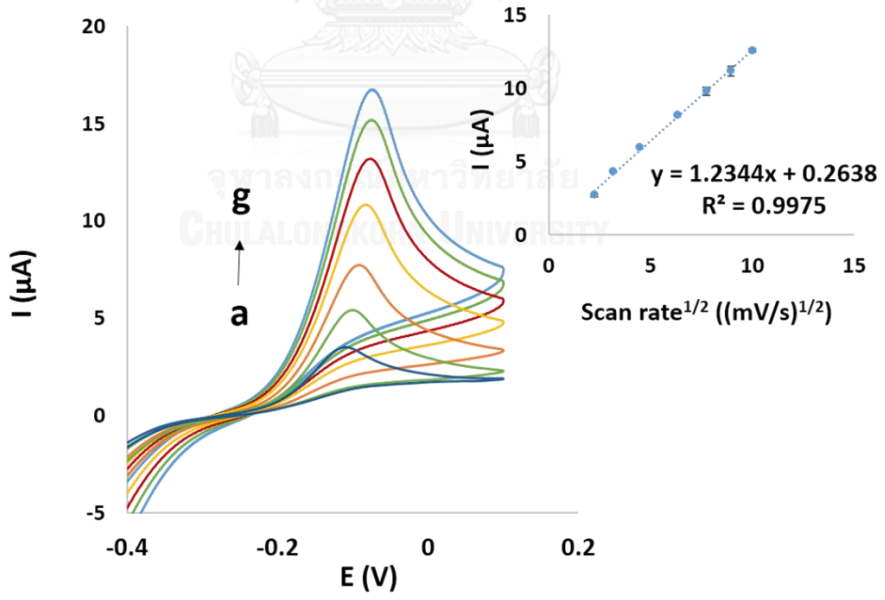

Figure 4.12 Cyclic voltammograms of 0.1 mM hydrazine in 0.1 M PBS (pH 7.0) measured on NG-PVP/AuNPs modified SPCE at different scan rates of 5, 10, 20, 40, 60, 80, 100 mV s^{-1} (a-g) and the anodic peak current of hydrazine as a function of square root of scan rate ($\mathbf{V}^{1/2}$) (inset).

4.2.3 Electrocatalytic oxidation of hydrazine at different electrodes

Figure 4.13 showed cyclic voltammograms of 0.5 mM hydrazine in 0.1 M PBS (pH 7.0) measured on different electrodes including unmodified SPCE (a), NG-PVP modified SPCE (b) and NG-PVP/AuNPs modified SPCE (c). The unmodified SPCE (a) exhibited the poor current response and no oxidation peak of hydrazine oxidation. After the SPCE was modified with NG-PVP nanocomposite, the NG-PVP modified SPCE (b) exhibited 4-time higher in anodic peak current than unmodified SPCE (a). Interestingly, when the AuNPs was electrodeposited on the NG-PVP nanocomposite, the large negative shift and well-formed sharp peak were observed (c). The catalytic peak current obtained from NG-PVP/AuNPs modified SPCE at the oxidation potential of 0.003 V showed the highest response, which was higher than unmodified SPCE for 10 times. The substantial increase of current and large decrease of oxidation potential clearly indicate that NG-PVP/AuNPs nanocomposite can effectively accelerate the electron transfer of the modified SPCE and shows an excellent electrocatalytic activity towards hydrazine oxidation. Thus, NG-PVP/AuNPs modified SPCE is a promising electrochemical sensor for sensitive determination of hydrazine.

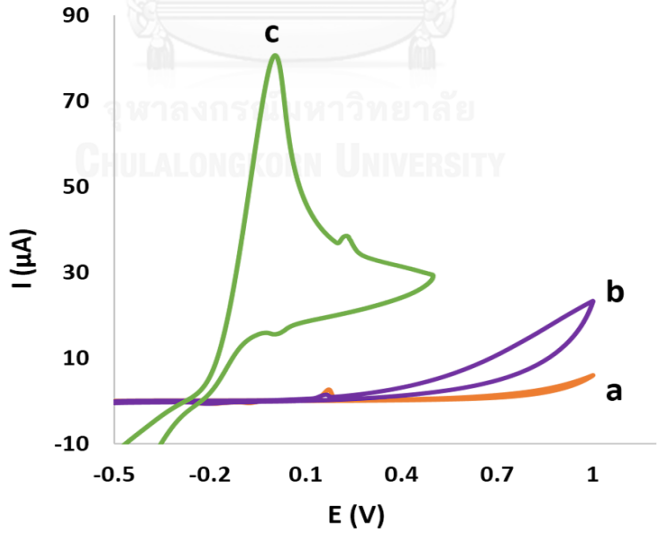

Figure 4.13 Cyclic voltammograms of 0.5 mM hydrazine in 0.1 M PBS (pH 7.0) with scan rate of 100 mV s^{-1} obtained at unmodified SPCE (a), NG-PVP modified SPCE (b), and NG-PVP/AuNPs modified SPCE (c).

4.2.4 Parameter optimization for square wave voltammetric determination of hydrazine

Due to the high electrochemical sensitivity of our system, it was applied for hydrazine determination using SWV. To obtain the highest current response for hydrazine detection, SWV parameters including step potential, amplitude and frequency were optimized using 50 μM hydrazine in 0.1 M PBS (pH 7.0) on NG-PVP/AuNPs modified SPCE. The selection of optimum conditions was based on the compromise of high current response, narrow peak shape and low background current. As shown in the Figure 4.14A, at 16 mV of step potential, the current response was high and the well-defined peak shape was obtained, so a step potential of 16 mV was selected. For amplitude (Figure 4.14B), the current response seems to be constant from 80-120 mV, however, the broader peaks were obtained at 100 and 120 mV; thus, 80 mV of amplitude was chosen. Figure 4.14C showed a highest response at 15 Hz of frequency. At higher frequency, the peak responses were obtained with higher background current, thus, frequency of 15 Hz was selected. Therefore, optimal conditions for SWV parameters were a step potential of 16 mV, an amplitude of 80 mV and a frequency of 15 Hz and these conditions will be used for further experiments.

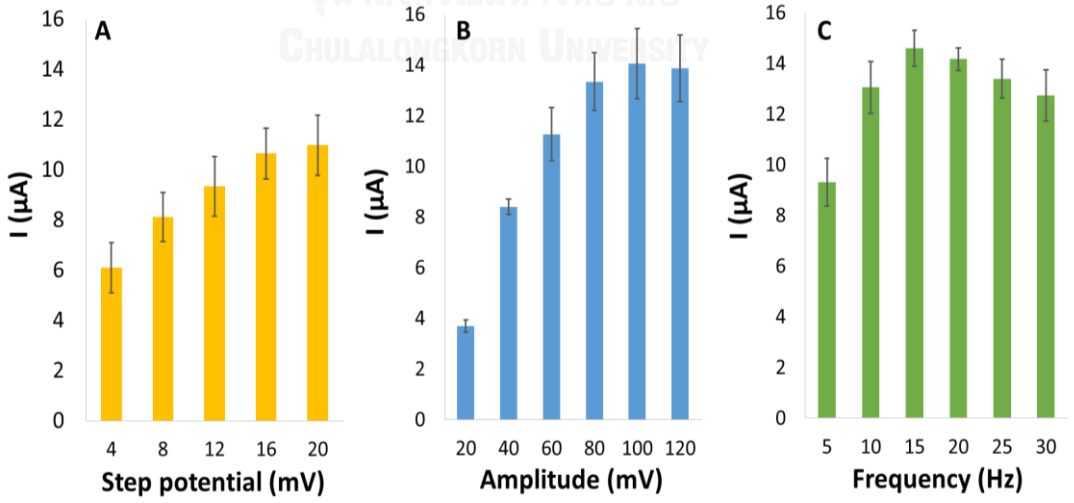

Figure 4.14 Anodic current responses obtained from square wave voltammetric measurement (SWV) of 50 μM hydrazine in 0.1 M PBS (pH 7.0) using NG-PVP/AuNPs modified SPCE with different step potential (A), amplitude (B) and frequency (C).

4.2.5 Analytical performances of NG-PVP/AuNPs modified SPCE for hydrazine determination

Under optimum conditions, the analytical performances of NG-PVP/AuNPs modified SPCE toward hydrazine detection were investigated by SWV. The inset of Figure 4.15 showed that the anodic peak current linearly increased as a function of concentration of hydrazine over a range from 2–300 μM with a correlation coefficient (R^2) of 0.9941. The limit of detection (LOD) was calculated using the following equation; LOD = $3S_b/m$, where S_b is a standard deviation of a signal obtained from a blank solution (seven-time determinations), m is a slope of calibration curve. The detection limit of hydrazine was found to be 68 nM with a sensitivity of 1.370 μAμM^{-1} cm^{-2}.

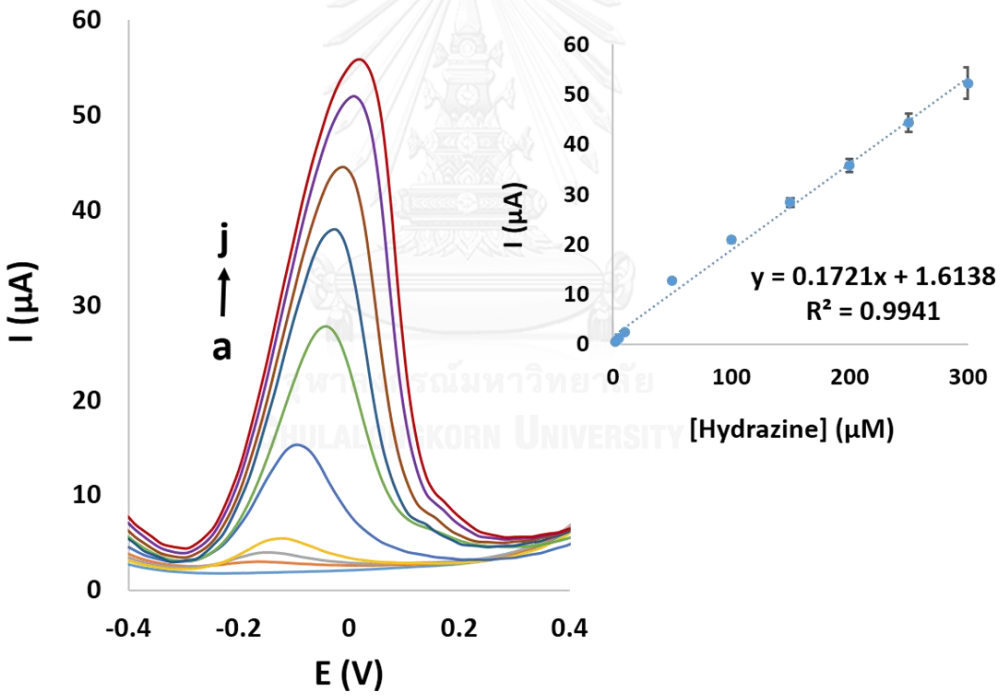

Figure 4.15 Square wave voltammograms (SWVs) of hydrazine over the concentration range of 0, 2, 5, 10, 50, 100, 150, 200, 250 and 300 μM (a-j) in 0.1 M PBS (pH 7.0) and a calibration plot between the hydrazine concentration (2-300 μM) and current response (inset) using NG-PVP/AuNPs modified SPCE.

The analytical performances of the proposed method were compared with the previously reports for hydrazine sensors as shown in Table 4.1. It can be seen that our proposed system exhibits low LOD, high sensitivity and a comparable linear range for the hydrazine detection. These results confirm that NG-PVP/AuNPs modified SPCE might be an alternative tool for hydrazine detection.

Table 4.1 Comparison of analytical performances for the hydrazine determination by using various modified electrodes.

Modified electrode	Method	E_p (V)	LOD (μM)	Linear range (μM)	Sensitivity	Refs.
Curcumin/MWCNTs/GCE	Amperometry	0.25	1.4	2-44	0.0229 μA μM^{-1}	[65]
AgNCs-PVP/GCE	Amperometry	0.4	1.1	5-460	-	[62]
Nano-Au/Ti	Amperometry	-0.55	42	500-4000	1.117 μA μM^{-1}	[66]
AuNPs/Poly(BCP)/CNTs/GCE	LSV	-0.028	0.1	0.5-1000	-	[67]
G/CCLP-AuNPs/GCE	Amperometry	0.1	0.0016	0.01-0.6	47.6 nA nM^{-1} cm^{-2}	[61]
			0.1	0.6-197.4	1.786 μA μM^{-1} cm^{-2}	
AuNPs/GPE	Amperometry	0.3	3.07	25-1000	-	[22]
	SWV		0.042	0.05-1000		
G-PANI/FTO	I-V characteristic	0.35	15380	0.01-100	0.325 μA μM^{-1} cm^{-2}	[68]
Nanoporous Au/ITO	Amperometry	0.2	0.0044	0.005-2050	0.1606 μA μM^{-1}	[69]
AgNPs/PPy/GCE	CV	0.3	0.2	0.5-1000	0.0114 μA μM^{-1}	[16]
				1000-10000		
Nano-Au/ZnO-MWCNTs/GCE	Amperometry	0.21	0.15	0.5-1800	0.0428 μA μM^{-1}	[41]
NG-PVP/AuNPs/SPCE	SWV	0.003	0.068	2-300	1.370 μA μM^{-1} cm^{-2}	This work
					(0.1721 μA μM^{-1})	

Abbreviations: GCE, glassy carbon electrode; GPE, graphite pencil electrode; SPCE, screen-printed carbon electrode; FTO, fluorinated tin oxide glass; MWCNTs, multi-walled carbon nanotubes; AgNCs, silver nanocubes; PVP, polyvinylpyrrolidone; AuNPs, gold nanoparticles; Poly(BCP), poly(bromocresol purple); G, graphene; NG, nitrogen-doped graphene; CCLP, calcium cross linked pectin; ZnO, Zinc oxide; PPy, polypyrrole; LSV, linear sweep voltammetry; CV, cyclic voltammetry; SWV, square wave voltammetry. [65] [66] [67] [61] [22] [68] [69]

4.2.6 Repeatability and reproducibility

Repeatability and reproducibility of NG-PVP/AuNPs modified SPCE were examined by SWV measurements of 50 μM hydrazine in 0.1 M PBS (pH 7.0). The percentage of relative standard deviation (%RSD) obtained from ten consecutive scans measuring on the same electrode, was found to be 3.69%. For the fabrication reproducibility, five independently fabricated modified SPCEs showed an acceptable reproducibility with the %RSD of 4.76. These results verify that this system has a good repeatability and reproducibility toward hydrazine detection.

4.2.7 Interference study

The selectivity of the fabricated hydrazine sensor was investigated by determination of 50 μM hydrazine in the presence of different interferences. In this study, the tolerance limit is defined as the molar ratio of potential interferences/hydrazine that caused the ±5% change in the current response of hydrazine. For the detection of hydrazine oxidation against potential interferences, the tolerance limits of all interferences were summarized as shown in the Table 4.2. It can be noticed that there is no interfering effect for most of interference species. Particularly, the high level of sugars (*i.e.* glucose, sucrose and lactose) did not interfere in the determination of hydrazine on NG-PVP/AuNPs modified SPCE. Thus, this system might be a promising tool for the determination of hydrazine in high sugar fruits and vegetables.

Table 4.2 The tolerance limit of potential interferences for the determination of hydrazine using the NG-PVP/AuNPs modified SPCE

Interferences	Tolerance limit (Fold)
K^+, Na^+, Mg^{2+}, Ca^{2+}, Zn^{2+}	125
NO_3^-, SO_4^{2-}	125
Fe^{3+}	10
Glucose, Sucrose, Lactose	750

However, when the concentrations of the interferences were higher than their tolerance limits, the current responses were decreased which is probably caused by obstructing hydrazine oxidation at the electrode surface by interference ions. The SWVs of hydrazine mixed with the interferences were shown in Appendixes.

4.2.8 Real sample analysis

To evaluate the method applicability, NG-PVP/AuNPs modified SPCE was used to measure the concentration of hydrazine in fruit and vegetable samples using a standard addition method. The 20-time diluted sugarcane, 20-time diluted sapodilla and 100-time diluted sweet corn juices were spiked with standard hydrazine to obtain the final hydrazine concentrations of 10, 50 and 100 μM. Each sample was individually measured for three times under the optimized SWV conditions and the results were summarized in Table 4.3. The percentages of recoveries were found in a range from 91.96–107.4% and the acceptable %RSD (n=3) was below 7%. These results verify the practical applicability of NG-PVP/AuNPs modified SPCE for the determination of hydrazine in high sugar fruit and vegetable samples with satisfactory results.

Table 4.3 Determination of hydrazine in fruit and vegetable samples using the NG-PVP/AuNPs modified SPCE (n=3).

Samples	Concentration of hydrazine		Recovery (%)	RSD (%)
	Added (μM)	Found (μM)		
Sugarcane	10	10.11 ± 0.05	101.07	4.93
	50	52.60 ± 2.58	105.20	4.91
	100	105.19 ± 6.50	105.19	6.18
Sapodilla	10	10.38 ± 0.27	103.78	2.60
	50	51.66 ± 2.36	103.32	4.56
	100	107.40 ± 1.72	107.40	1.60
Sweet corn	10	10.09 ± 0.33	100.90	3.31
	50	48.80 ± 1.97	97.59	4.05
	100	91.96 ± 3.73	91.96	4.06

CHAPTER V
CONCLUSIONS

5.1 Conclusions

G nanocomposite modified screen-printed carbon electrodes (SPCEs) were developed as novel electrochemical sensors for the determination of target analytes. The details in the development of electrochemical sensor were summarized as follows:

5.1.1 Graphene-Polyvinylpyrrolidone /Polyaniline nanocomposite modified electrode for the determination of cholesterol

An electrochemical sensor based on G-PVP/PANI modified SPCE was developed for the determination of H_2O_2 and cholesterol. The G-PVP/PANI modified electrode exhibited much higher electrochemical sensitivity for H_2O_2 detection compared to an unmodified electrode. However, there were some problems that caused the abrogation of the system involved in cholesterol biosensor. Therefore, the new system were developed and applied for new target analyte.

5.1.2 Nitrogen-Doped Graphene-Polyvinylpyrrolidone/Gold Nanoparticles Modified Electrode as a Novel Hydrazine Sensor

NG-PVP/AuNPs modified SPCEs were firstly prepared via electrospraying of NG-PVP coupled with AuNPs electrodeposition for square wave voltammetric determination of hydrazine. The electrode composition and SWV parameters were investigated and optimized**.** The fabricated sensor exhibited higher electrochemical sensitivity and a higher electrocatalytic activity toward the oxidation of hydrazine compared to an unmodified SPCE. Under the optimal conditions, a low LOD of 68 nM, a linear range of 2-300 μM, and a high sensitivity of 1.370 μA μM^{-1} cm^{-2} were achieved for hydrazine. Moreover, the developed hydrazine sensor was highly selective against the potential interferences. Finally, the purposed system was successfully applied for the hydrazine determination in high sugar fruit and vegetable samples with the percentage of recoveries ranging from 91.69-107.40%.

5.2 Suggestion works

Due to the good analytical performances, large surface area and good biocompatibility of NG-PVP/AuNPs modified SPCE, the fabricated sensor might be further studied and applied for the development of electrochemical biosensor which is involved in biofunctionalization on the modified electrode surface.

REFERENCES

[1] Charoenkitamorn, K., Chailapakul, O., and Siangproh, W. Development of gold nanoparticles modified screen-printed carbon electrode for the analysis of thiram, disulfiram and their derivative in food using ultra-high performance liquid chromatography. Talanta 132(0) (2015): 416-423.

[2] Guan, W.J., Li, Y., Chen, Y.Q., Zhang, X.B., and Hu, G.Q. Glucose biosensor based on multi-wall carbon nanotubes and screen printed carbon electrodes. Biosensors and Bioelectronics 21(3) (2005): 508-512.

[3] Liu, Y., Dong, X., and Chen, P. Chemical Society Reviews 41(0) (2012): 2283-2307.

[4] Dey, R.S. and Raj, C.R. Development of an Amperometric Cholesterol Biosensor Based on Graphene-Pt Nanoparticle Hybrid Material. The Journal of Physical Chemistry C 114(0) (2010): 21427–21433.

[5] Cao, S., Zhang, L., Chai, Y., and Yuan, R. Electrochemistry of cholesterol biosensor based on a novel Pt-Pd bimetallic nanoparticle decorated graphene catalyst. Talanta 109(0) (2013): 167-172.

[6] Pakapongpan, S., Mensing, J.P., Phokharatkul, D., Lomas, T., and Tuantranont, A. Highly selective electrochemical sensor for ascorbic acid based on a novel hybrid graphene-copper phthalocyanine-polyaniline nanocomposites. Electrochimica Acta 133 (2014): 294-301.

[7] Manjunatha, R., Shivappa Suresh, G., Melo, J.S., D'Souza, S.F., and Venkatesha, T.V. An amperometric bienzymatic cholesterol biosensor based on functionalized graphene modified electrode and its electrocatalytic activity towards total cholesterol determination. Talanta 99(0) (2012): 302-309.

[8] Parlak, O., Tiwari, A., and Turner, A.P. Template-directed hierarchical self-assembly of graphene based hybrid structure for electrochemical biosensing. Biosensors and Bioelectronics 49 (2013): 53-62.

[9] Liu, S., Xing, X., Yu, J., Lian, W., Li, J., Cui, M., and Huang, J. A novel label-free electrochemical aptasensor based on graphene-polyaniline composite film for dopamine determination. Biosensors and Bioelectronics 36(1) (2012): 186-191.

[10] Wang, Y., Shao, Y., Matson, D.W., Li, J., and Lin, Y. Nitrogen-Doped Graphene and Its Application in Electrochemical Biosensing. ACS Nano 4(4) (2010): 1790–1798.

[11] Sheng, Z.-H., Shao, L., Chen, J.-J., Bao, W.-J., Wang, F.-B., and Xia, X.-H. Catalyst-Free Synthesis of Nitrogen-Doped Graphene via Thermal Annealing Graphite Oxide with Melamine and Its Excellent Electrocatalysis. ACS Nano 5(6) (2011): 4350-4358.

[12] Li, D., Muller, M.B., Gilje, S., Kaner, R.B., and Wallace, G.G. Processable aqueous dispersions of graphene nanosheets. Nature Nanotechnology 3(2) (2008): 101-105.

[13] Wajid, A.S., Das, S., Irin, F., Ahmed, H.S.T., Shelburne, J.L., Parviz, D., Fullerton, R.J., Jankowski, A.F., Hedden, R.C., and Green, M.J. Polymer-stabilized graphene dispersions at high concentrations in organic solvents for composite production. Carbon 50(2) (2012): 526-534.

[14] Shan, C., Yang, H., Song, J., Han, D., Ivaska, A., and Niu, L. Direct Electrochemistry of Glucose Oxidase and Biosensing for Glucose Based on Graphene. Analytical Chemistry 81(6) (2009): 2378-2382.

[15] Dhand, C., Das, M., Datta, M., and Malhotra, B.D. Recent advances in polyaniline based biosensors. Biosensors and Bioelectronics 26(6) (2011): 2811-2821.

[16] Ghanbari, K. Fabrication of silver nanoparticles–polypyrrole composite modified electrode for electrocatalytic oxidation of hydrazine. Synthetic Metals 195(0) (2014): 234-240.

[17] Arya, S.K., Dey, A., and Bhansali, S. Polyaniline protected gold nanoparticles based mediator and label free electrochemical cortisol biosensor. Biosensors and Bioelectronics 28(1) (2011): 166-173.

[18] Bernalte, E., Marín Sánchez, C., and Pinilla Gil, E. Gold nanoparticles-modified screen-printed carbon electrodes for anodic stripping voltammetric

determination of mercury in ambient water samples. Sensors and Actuators B: Chemical 161(1) (2012): 669-674.

[19] Pruneanu, S., Pogacean, F., Biris, A.R., Ardelean, S., Canpean, V., Blanita, G., Dervishi, E., and Biris, A.S. Novel Graphene-Gold Nanoparticle Modified Electrodes for the High Sensitivity Electrochemical Spectroscopy Detection and Analysis of Carbamazepine. The Journal of Physical Chemistry C 115(47) (2011): 23387-23394.

[20] Fan, Y., Liu, J.-H., Yang, C.-P., Yu, M., and Liu, P. Graphene–polyaniline composite film modified electrode for voltammetric determination of 4-aminophenol. Sensors and Actuators B: Chemical 157(2) (2011): 669-674.

[21] Bardpho, C., Rattanarat, P., Siangproh, W., and Chailapakul, O. Ultra-high performance liquid chromatographic determination of antioxidants in teas using inkjet-printed graphene–polyaniline electrode. Talanta (0).

[22] Abdul Aziz, M. and Kawde, A.N. Gold nanoparticle-modified graphite pencil electrode for the high-sensitivity detection of hydrazine. Talanta 115 (2013): 214-221.

[23] Jia, W., Su, L., and Lei, Y. Pt nanoflower/polyaniline composite nanofibers based urea biosensor. Biosensors and Bioelectronics 30(1) (2011): 158-64.

[24] Rodthongkum, N., Ruecha, N., Rangkupan, R., Vachet, R.W., and Chailapakul, O. Graphene-loaded nanofiber-modified electrodes for the ultrasensitive determination of dopamine. Analytica Chimica Acta 804(0) (2013): 84-91.

[25] Marx, S., Jose, M.V., Andersen, J.D., and Russell, A.J. Electrospun gold nanofiber electrodes for biosensors. Biosensors and Bioelectronics 26(6) (2011): 2981-2986.

[26] Ruecha, N., Rangkupan, R., Rodthongkum, N., and Chailapakul, O. Novel paper-based cholesterol biosensor using graphene/polyvinylpyrrolidone/polyaniline nanocomposite. Biosensors and Bioelectronics 52 (2014): 13-19.

[27] Thammasoontaree, N., Rattanarat, P., Ruecha, N., Siangproh, W., Rodthongkum, N., and Chailapakul, O. Ultra-performance liquid chromatography coupled with graphene/polyaniline nanocomposite modified

electrode for the determination of sulfonamide residues. Talanta 123 (2014): 115-21.

[28] Wang, J. Analytical Electrochemistry. 2 ed. the United staes of America: Wiley-VCH, 2000.

[29] Bard, A.J.a.F., L.R. . Electrochemical methods : fundamentals and applications. 2 ed. the United States of America: John Wiley & Sons, Inc, 2001.

[30] Macdonald, D.D. Reflections on the history of electrochemical impedance spectroscopy. Electrochimica Acta 51(8–9) (2006): 1376-1388.

[31] Dornbusch, D.A., Hilton, R., Gordon, M.J., and Suppes, G.J. Effects of Sonication on EIS Results for Zinc Alkaline Batteries. ECS Electrochemistry Letters 2(9) (2013): A89-A92.

[32] Li, M., Li, Y.-T., Li, D.-W., and Long, Y.-T. Recent developments and applications of screen-printed electrodes in environmental assays—A review. Analytical Chimica Acta 734(0) (2012): 31-44.

[33] Metters, J.P. and Banks, C.E. Screen Printed Electrodes Open New Vistas in Sensing: Application to Medical Diagnosis. in Schlesinger, M. (ed.) Applications of Electrochemistry in Medicine. the United states of America: Springer Science+Business Media, 2013.

[34] Kuila, T., Bose, S., Khanra, P., Mishra, A.K., Kim, N.H., and Lee, J.H. Recent advances in graphene-based biosensors. Biosensors and Bioelectronics 26(12) (2011): 4637-4648.

[35] Singh, K., Solanki, P.R., Basu, T., and Malhotra, B.D. Polypyrrole/multiwalled carbon nanotubes-based biosensor for cholesterol estimation. Polymers for Advanced Technologies 23(7) (2012): 1084-1091.

[36] Wilson, J., Radhakrishnan, S., Sumathi, C., and Dharuman, V. Polypyrrole–polyaniline–Au (PPy–PANi–Au) nano composite films for label-free electrochemical DNA sensing. Sensors and Actuators B: Chemical 171-172 (2012): 216-222.

[37] Jiang, F., Yue, R., Du, Y., Xu, J., and Yang, P. A one-pot 'green' synthesis of Pd-decorated PEDOT nanospheres for nonenzymatic hydrogen peroxide sensing. Biosensors and Bioelectronics 44 (2013): 127-131.

[38] Karuwan, C., Sriprachuabwong, C., Wisitsoraat, A., Phokharatkul, D., Sritongkham, P., and Tuantranont, A. Inkjet-printed graphene-poly(3,4-ethylenedioxythiophene):poly(styrene-sulfonate) modified on screen printed carbon electrode for electrochemical sensing of salbutamol. Sensors and Actuators B: Chemical 161(1) (2012): 549-555.

[39] Ruecha, N., Rangkupan, R., Rodthongkum, N., and Chailapakul, O. Novel paper-based cholesterol biosensor using graphene/polyvinylpyrrolidone/polyaniline nanocomposite. Biosensors and Bioelectronics 52(0) (2014): 13-19.

[40] Hernández-Santos, D., González-García, M.B., and García, A.C. Metal-Nanoparticles Based Electroanalysis. Electroanalysis 14(18) (2002): 1225-1235.

[41] Zhang, C., Wang, G., Ji, Y., Liu, M., Feng, Y., Zhang, Z., and Fang, B. Enhancement in analytical hydrazine based on gold nanoparticles deposited on ZnO-MWCNTs films. Sensors and Actuators B: Chemical 150(1) (2010): 247-253.

[42] Arya, N., Chakraborty, S., Dube, N., and Katti, D.S. Electrospraying: A facile technique for synthesis of chitosan-based micro/nanospheres for drug delivery applications. Journal of Biomedical Materials Research Part B: Applied Biomaterials 88B(1) (2009): 17-31.

[43] Gaskell, S.J. Electrospray: Principles and Practice. Journal of Mass Spectrometry 32(7) (1997): 677-688.

[44] Low, C.T.J., Wills, R.G.A., and Walsh, F.C. Electrodeposition of composite coatings containing nanoparticles in a metal deposit. Surface and Coatings Technology 201(1–2) (2006): 371-383.

[45] Arya, S.K., Datta, M., and Malhotra, B.D. Recent advances in cholesterol biosensor. Biosensors and Bioelectronics 23(7) (2008): 1083-1100.

[46] Chaubey, A. and Malhotra, B.D. Mediated biosensors. Biosensors and Bioelectronics 17(6–7) (2002): 441-456.

[47] Singh, S., Solanki, P.R., Pandey, M.K., and Malhotra, B.D. Cholesterol biosensor based on cholesterol esterase, cholesterol oxidase and peroxidase immobilized onto conducting polyaniline films. Sensors and Actuators B: Chemical 115(1) (2006): 534-541.

[48] Shih, W.-C., Yang, M.-C., and Lin, M.S. Development of disposable lipid biosensor for the determination of total cholesterol. Biosensors and Bioelectronics 24(6) (2009): 1679-1684.

[49] Soylemez, S., Ekiz Kanik, F., Ileri, M., Hacioglu, S.O., and Toppare, L. Development of a novel biosensor based on a conducting polymer. Talanta 118(0) (2014): 84-89.

[50] Solanki, P.R., Kaushik, A., Ansari, A.A., Tiwari, A., and Malhotra, B.D. Multi-walled carbon nanotubes/sol–gel-derived silica/chitosan nanobiocomposite for total cholesterol sensor. Sensors and Actuators B: Chemical 137(2) (2009): 727-735.

[51] Yamada, K., Yasuda, K., Fujiwara, N., Siroma, Z., Tanaka, H., Miyazaki, Y., and Kobayashi, T. Potential application of anion-exchange membrane for hydrazine fuel cell electrolyte. Electrochemistry Communications 5(10) (2003): 892-896.

[52] Amlathe, S. and Gupta, V.K. Spectrophotometric determination of trace amounts of hydrazine in polluted water. Analyst 113(9) (1988): 1481-1483.

[53] Ortega-Barrales, P., Molina-Díaz, A., Pascual-Reguera, M.I., and Capitán-Vallvey, L.F. Solid-phase spectrophotometric determination of trace amounts of hydrazine at sub-ng ml−1 level. Analytica Chimica Acta 353(1) (1997): 115-122.

[54] Plunkett, S., Parrish, M.E., Shafer, K.H., Shorter, J.H., Nelson, D.D., and Zahniser, M.S. Hydrazine detection limits in the cigarette smoke matrix using infrared tunable diode laser absorption spectroscopy. Spectrochimica Acta Part A 58(11) (2002): 2505-2517.

[55] Safavi, A. and Karimi, M.A. Flow injection chemiluminescence determination of hydrazine by oxidation with chlorinated isocyanurates. Talanta 58(4) (2002): 785-792.

[56] Ensafi, A.A. and Rezaei, B. Flow injection determination of hydrazine with fluorimetric detection. Talanta 47(3) (1998): 645-649.

[57] Smolenkov, A.D. and Shpigun, O.A. Direct liquid chromatographic determination of hydrazines: A review. Talanta 102(0) (2012): 93-100.

[58] Sun, M., Bai, L., and Liu, D.Q. A generic approach for the determination of trace hydrazine in drug substances using in situ derivatization-headspace GC–MS. Journal of Pharmaceutical and Biomedical Analysis 49(2) (2009): 529-533.

[59] Oh, J.-A., Park, J.-H., and Shin, H.-S. Sensitive determination of hydrazine in water by gas chromatography–mass spectrometry after derivatization with ortho-phthalaldehyde. Analytica Chimica Acta 769(0) (2013): 79-83.

[60] Li, J. and Lin, X. Electrocatalytic oxidation of hydrazine and hydroxylamine at gold nanoparticle—polypyrrole nanowire modified glassy carbon electrode. Sensors and Actuators B: Chemical 126(2) (2007): 527-535.

[61] Devasenathipathy, R., Mani, V., Chen, S.-M., Arulraj, D., and Vasantha, V.S. Highly stable and sensitive amperometric sensor for the determination of trace level hydrazine at cross linked pectin stabilized gold nanoparticles decorated graphene nanosheets. Electrochimica Acta 135 (2014): 260-269.

[62] Wang, Y., Yang, X., Bai, J., Jiang, X., and Fan, G. High sensitivity hydrogen peroxide and hydrazine sensor based on silver nanocubes with rich {100} facets as an enhanced electrochemical sensing platform. Biosensors and Bioelectronics 43 (2013): 180-185.

[63] Kim, S.P. and Choi, H.C. Reusable hydrazine amperometric sensor based on Nafion®-coated TiO2–carbon nanotube modified electrode. Sensors and Actuators B: Chemical 207 (2015): 424-429.

[64] Singh, S., Solanki, P.R., Pandey, M.K., and Malhotra, B.D. Covalent immobilization of cholesterol esterase and cholesterol oxidase on polyaniline films for application to cholesterol biosensor. Analytica Chimica Acta 568(1-2) (2006): 126-132.

[65] Zheng, L. and Song, J.-f. Curcumin multi-wall carbon nanotubes modified glassy carbon electrode and its electrocatalytic activity towards oxidation of hydrazine. Sensors and Actuators B: Chemical 135(2) (2009): 650-655.

[66] Yi, Q. and Yu, W. Nanoporous gold particles modified titanium electrode for hydrazine oxidation. Journal of Electroanalytical Chemistry 633(1) (2009): 159-164.

[67] Koçak, S. and Aslışen, B. Hydrazine oxidation at gold nanoparticles and poly(bromocresol purple) carbon nanotube modified glassy carbon electrode. Sensors and Actuators B: Chemical 196 (2014): 610-618.

[68] Ameen, S., Akhtar, M.S., and Shin, H.S. Hydrazine chemical sensing by modified electrode based on in situ electrochemically synthesized polyaniline/graphene composite thin film. Sensors and Actuators B: Chemical 173 (2012): 177-183.

[69] Tang, Y.-Y., Kao, C.-L., and Chen, P.-Y. Electrochemical detection of hydrazine using a highly sensitive nanoporous gold electrode. Analytica Chimica Acta 711(0) (2012): 32-39.

APPENDIX

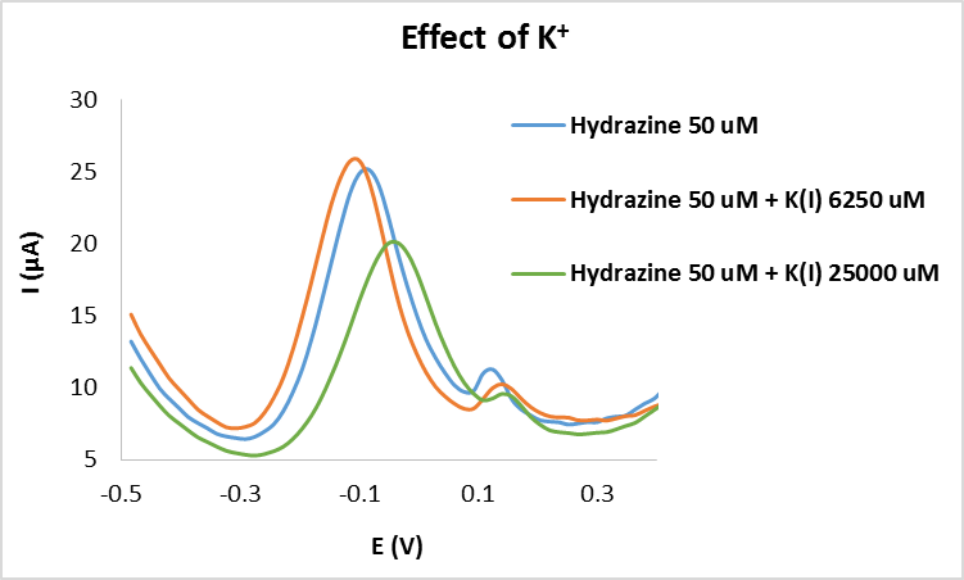

Figure S1 Square wave voltammograms (SWVs) of hydrazine mixed with KNO_3 in 0.1 M PBS (pH 7.0) using NG-PVP/AuNPs modified SPCE.

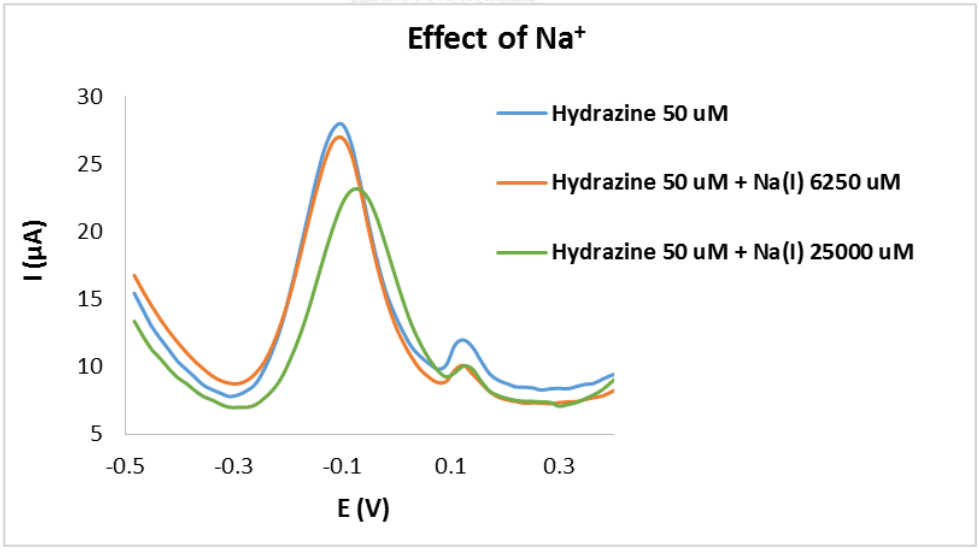

Figure S2 Square wave voltammograms (SWVs) of hydrazine mixed with Na_2SO_4 in 0.1 M PBS (pH 7.0) using NG-PVP/AuNPs modified SPCE.

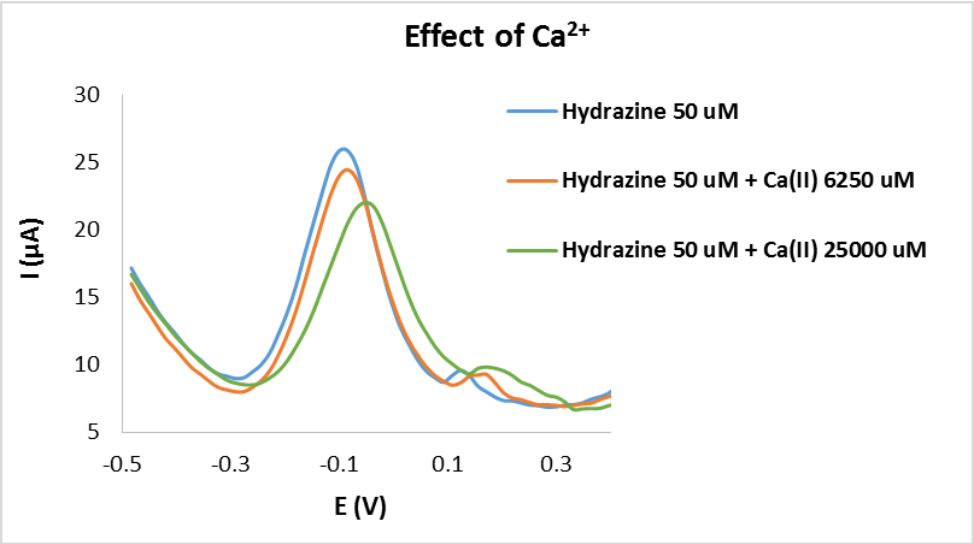

Figure S3 Square wave voltammograms (SWVs) of hydrazine mixed with $Ca(NO_3)_2$ in 0.1 M PBS (pH 7.0) using NG-PVP/AuNPs modified SPCE.

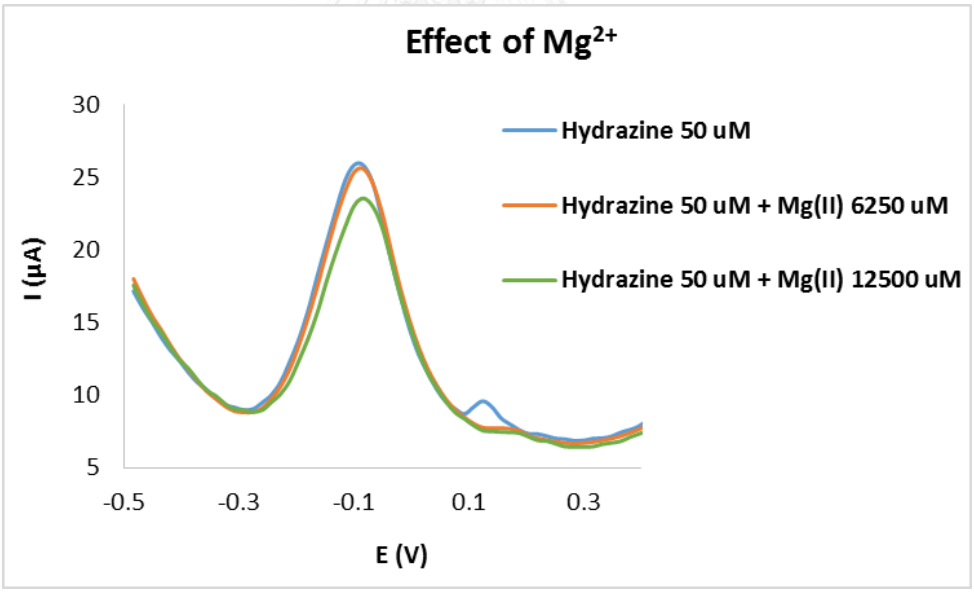

Figure S4 Square wave voltammograms (SWVs) of hydrazine mixed with $Mg(NO_3)_2$ in 0.1 M PBS (pH 7.0) using NG-PVP/AuNPs modified SPCE.

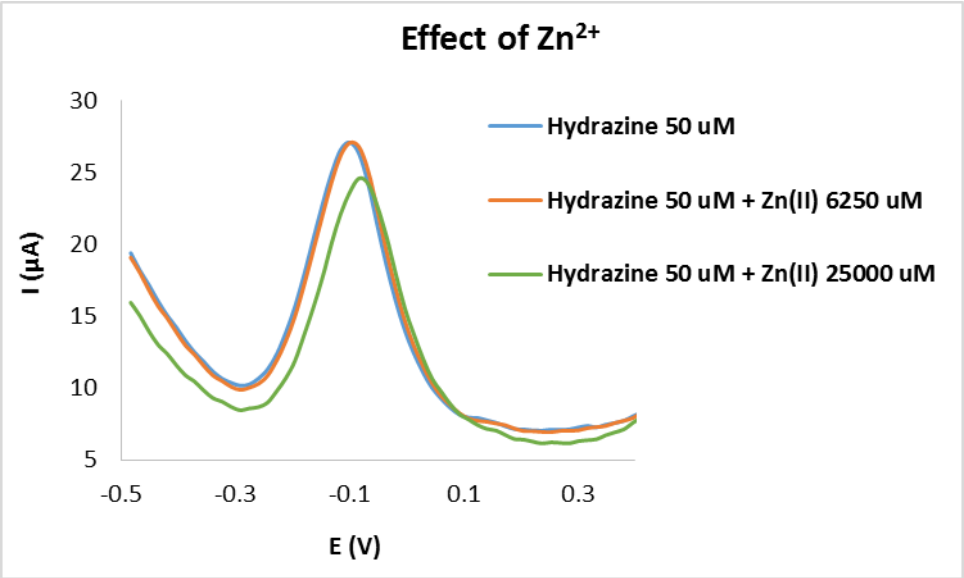

Figure S5 Square wave voltammograms (SWVs) of hydrazine mixed with $Zn(NO_3)_2$ in 0.1 M PBS (pH 7.0) using NG-PVP/AuNPs modified SPCE.

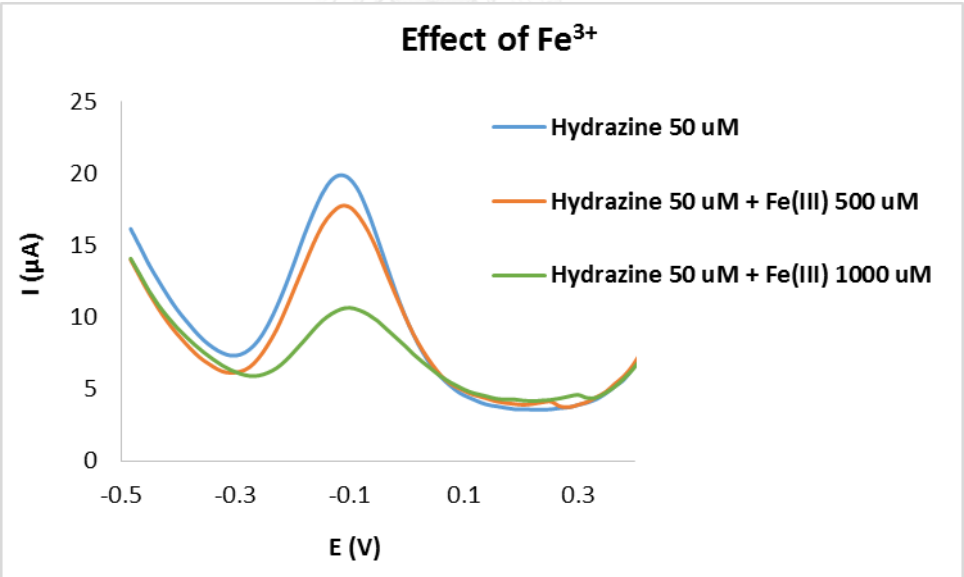

Figure S6 Square wave voltammograms (SWVs) of hydrazine mixed with $Fe_2(SO_4)_3$ in 0.1 M PBS (pH 7.0) using NG-PVP/AuNPs modified SPCE.

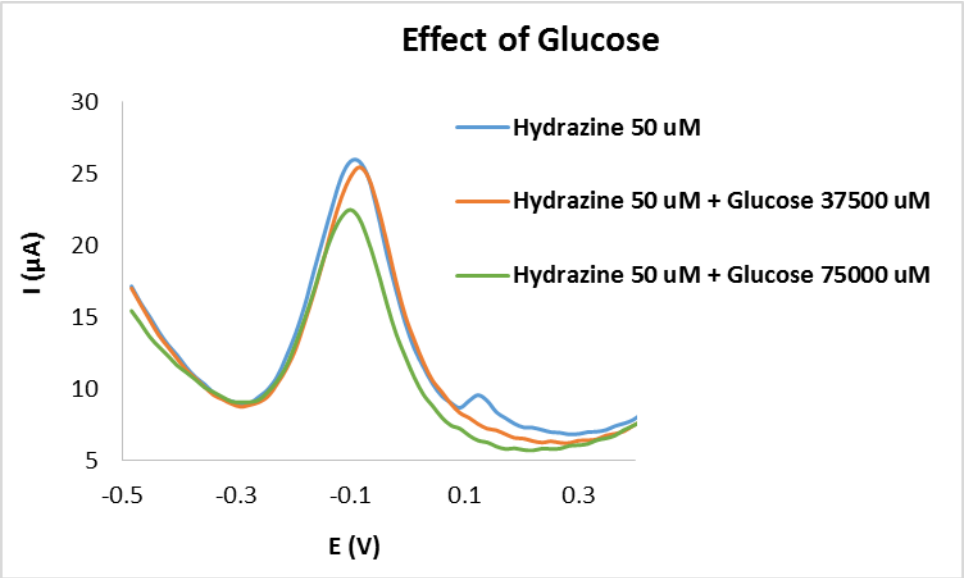

Figure S7 Square wave voltammograms (SWVs) of hydrazine mixed with glucose in 0.1 M PBS (pH 7.0) using NG-PVP/AuNPs modified SPCE.

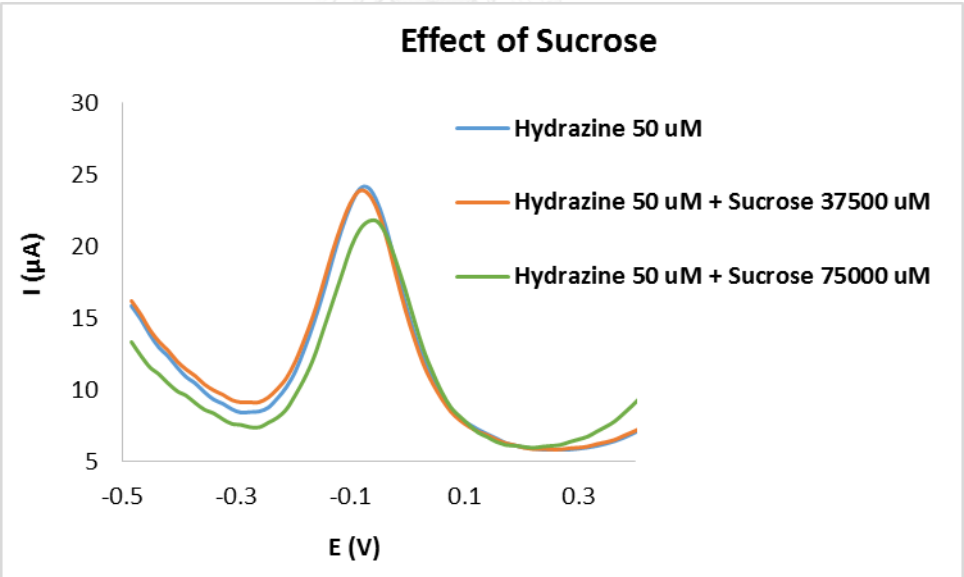

Figure S8 Square wave voltammograms (SWVs) of hydrazine mixed with sucrose in 0.1 M PBS (pH 7.0) using NG-PVP/AuNPs modified SPCE.

VITA

Chayada Saengsookwaow was born in November 25, 1988 in Sisaket, Thailand. She received her Bachelor Degree of Science, majoring in chemistry from Mahidol University, Bangkok, Thailand (2007-2011). She expect graduated her Mater Degree of Science, majoring in Petrochemistry and Polymer Science from Chulalongkorn University, Bangkok, Thailand in 2015.

Oral presentation

Chayada Saengsookwaow, Ratthapol Rangkupan, Nadnudda Rodthongkum, Orawan Chailapakul, “Graphene-polyaniline nanocomposite-based biosensor for cholesterol determination” Pure and Applied chemistry International Conference 2014 (PACCON2014), January 8-10, 2014, Khon Kaen, Thailand.

Proceeding

Chayada Saengsookwaow, Ratthapol Rangkupan, Nadnudda Rodthongkum, Orawan Chailapakul, “Graphene-polyaniline nanocomposite-based biosensor for cholesterol determination” Proceeding of Pure and Applied chemistry International Conference 2014. 2014: 405-408.